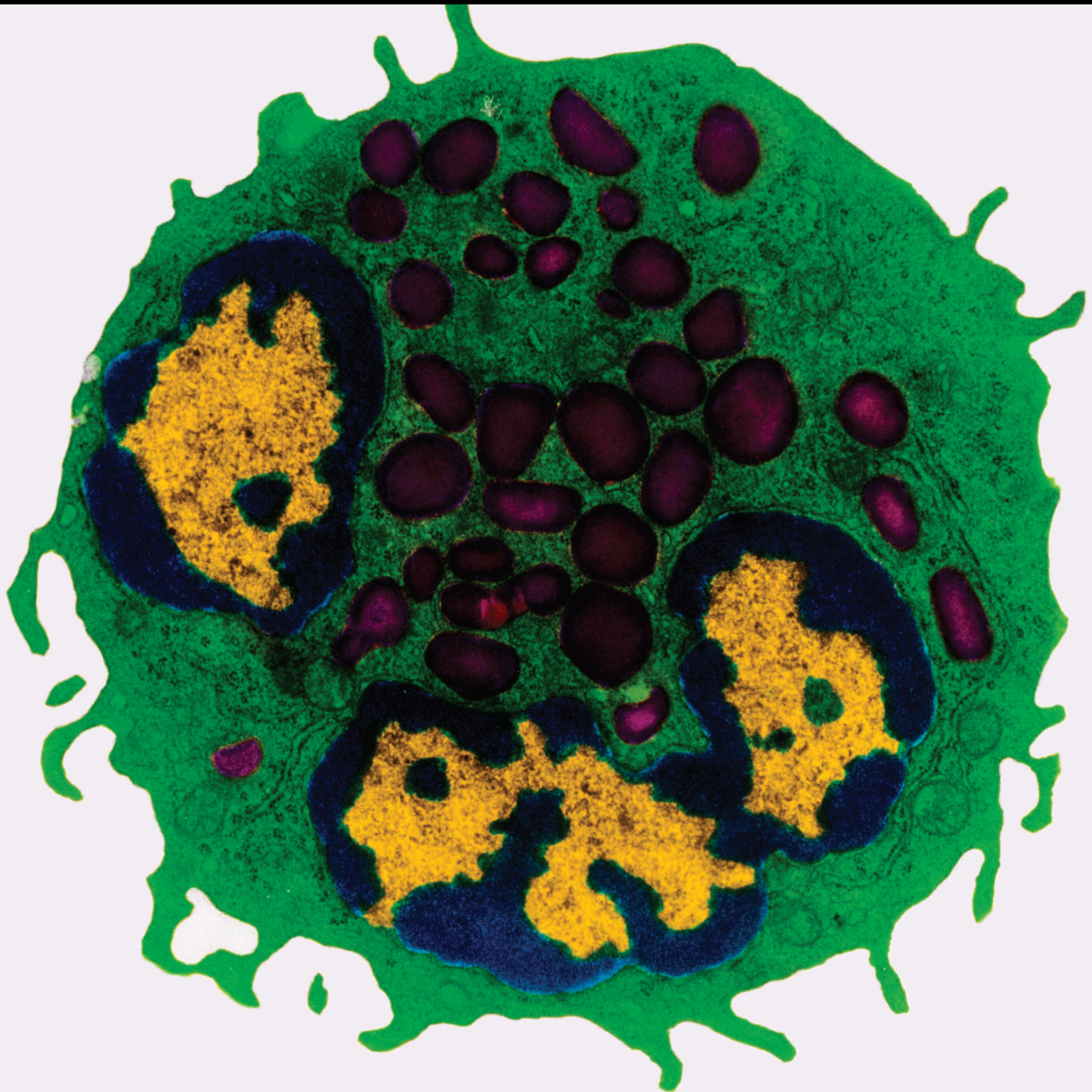# Hypoxia, Inflammation, and its Related Disorders

Lead Guest Editor: Javier Fernandez-Solari
Guest Editors: Paula Barrionuevo, María Victoria Aguirre, Jose Villacorta Hidalgo, Antonela Romina Terrizzi, and Maria Pilar Martinez

Hypoxia, Inflammation, and its Related Disorders

Hypoxia, Inflammation, and its Related Disorders

Lead Guest Editor: Javier Fernandez-Solari
Guest Editors: Paula Barrionuevo, María Victoria Aguirre, Jose Villacorta Hidalgo, Antonela Romina Terrizzi, and Maria Pilar Martinez

Chief Editor

Anshu Agrawal (iD), USA

Associate Editors

Carlo Cervellati (iD), Italy
Elaine Hatanaka (iD), Brazil
Vladimir A. Kostyuk (iD), Belarus
Carla Pagliari (iD), Brazil

Academic Editors

Amedeo Amedei (iD), Italy
Emiliano Antiga (iD), Italy
Tomasz Brzozowski (iD), Poland
Daniela Caccamo (iD), Italy
Luca Cantarini (iD), Italy
Raffaele Capasso (iD), Italy
Calogero Caruso (iD), Italy
Robson Coutinho-Silva (iD), Brazil
Jose Crispin (iD), Mexico
Fulvio D'Acquisto (iD), United Kingdom
Eduardo Dalmarco (iD), Brazil
Agnieszka Dobrzyn, Poland
Ulrich Eisel (iD), The Netherlands
Mirvat El-Sibai (iD), Lebanon
Giacomo Emmi (iD), Italy
Claudia Fabiani (iD), Italy
Fabíola B Filippin Monteiro (iD), Brazil
Antonella Fioravanti (iD), Italy
Tânia Silvia Fröde (iD), Brazil
Julio Galvez (iD), Spain
Mirella Giovarelli (iD), Italy
Denis Girard, Canada
Markus H. Gräler (iD), Germany
Oreste Gualillo (iD), Spain
Qingdong Guan (iD), Canada
Tommaso Iannitti (iD), United Kingdom
Byeong-Churl Jang, Republic of Korea
Yasumasa Kato (iD), Japan
Cheorl-Ho Kim (iD), Republic of Korea
Alex Kleinjan (iD), The Netherlands
Martha Lappas (iD), Australia
Ariadne Malamitsi-Puchner (iD), Greece
Palash Mandal, India
Joilson O. Martins (iD), Brazil
Donna-Marie McCafferty, Canada
Barbro N. Melgert (iD), The Netherlands

Paola Migliorini (iD), Italy
Vinod K. Mishra (iD), USA
Eeva Moilanen (iD), Finland
Elena Niccolai (iD), Italy
Nadra Nilsen (iD), Norway
Sandra Helena Penha Oliveira (iD), Brazil
Michal A. Rahat (iD), Israel
Zoltan Rakonczay Jr. (iD), Hungary
Marcella Reale (iD), Italy
Emanuela Roscetto, Italy
Domenico Sergi (iD), Italy
Mohammad Shadab (iD), USA
Elena Silvestri, Italy
Carla Sipert (iD), Brazil
Helen C. Steel (iD), South Africa
Saravanan Subramanian, USA
Veedamali S. Subramanian (iD), USA
Taina Tervahartiala, Finland
Alessandro Trentini (iD), Italy
Kathy Triantafilou, United Kingdom
Fumio Tsuji (iD), Japan
Maria Letizia Urban, Italy
Giuseppe Valacchi (iD), Italy
Kerstin Wolk (iD), Germany
Soh Yamazaki (iD), Japan
Young-Su Yi (iD), Republic of Korea
Shin-ichi Yokota (iD), Japan
Francesca Zimetti (iD), Italy

Contents

Research Article

IL-1β Impaired Diabetic Wound Healing by Regulating MMP-2 and MMP-9 through the p38 Pathway

Jiezhi Dai, Junjie Shen, Yimin Chai [ID], and Hua Chen [ID]

Department of Orthopedic Surgery, Shanghai Jiao Tong University Affiliated Sixth People's Hospital, Shanghai, China

Correspondence should be addressed to Yimin Chai; ymchai@sjtu.edu.cn and Hua Chen; chuadr@aliyun.com

Diabetes mellitus is one of the most prominent metabolic disorders in the world, and insulin resistance in diabetic patients leads to several complications including increased inflammation and delayed wound healing. Fibroblast migration and reepithelialization play a significant role in wound healing. In this study, we explored the effects of IL-1β signaling on proliferation and migration of human fibroblasts from diabetic wound tissues. We observed elevated levels of IL-1β in samples from diabetic patients when compared to normal wound tissues. At high concentrations, IL-1β inhibited cell proliferation and migration in *ex vivo* fibroblast cultures. Moreover, expression of matrix metalloproteinases (MMPs) was upregulated, and tissue inhibitor of metalloproteinases (TIMPs) was downregulated in diabetic wound tissues and cells. These effects were regulated by levels of IL-1β. Furthermore, IL-1β induced p38 phosphorylation thereby activating the p38 MAPK pathway that in turn regulated the expression of MMPs and TIMPs. Together, our study identifies a novel mechanism behind delayed wound closure in diabetes mellitus that involves IL-1β-dependent regulation of cell proliferation and migration.

1. Introduction

Diabetes mellitus is one of the most prevalent chronic diseases worldwide [1, 2]. In China, 11% of adults lived with diabetes in 2010 that amount to a total of 109.6 million individuals [3]. With a rapid increase in the prevalence of diabetes mellitus, complications such as diabetic ulcers have become major causes of deformity worldwide [4]. Of the different symptoms associated with diabetes, impaired wound healing is one of the most prominent effects observed in patients. Wound healing is an evolutionarily conserved process that involves spatial and temporal overlap of processes such as inflammation, coagulation, cellular proliferation, and extracellular matrix (ECM) remodeling [5–8].

Matrix metalloproteinases (MMPs) are ECM remodeling proteins that play a significant role in various stages of the wound healing process. A regulated metalloproteinase activation and inhibition cascade is triggered following injury for efficient wound closure [9]. Initially, MMPs are involved in the removal of devitalized tissue following which during the repair phase, MMPs contribute to angiogenesis, contraction of the wound matrix, migration of fibroblasts and keratinocytes, and epithelialization. Finally, they are also involved in the remodeling of newly synthesized connective tissue [9, 10]. MMP activity is regulated by small inhibitory proteins known as tissue inhibitor of metalloproteinases (TIMPs), which also contribute to the initiation of cell division and binding to the ECM as well as the inhibition of angiogenesis and the induction of apoptosis [11]. Hence, the balance between MMP and TIMP activity is crucial for effective wound healing [12, 13].

Serum levels of IL-1β are elevated in patients with diabetes [14]. Previous studies identified the contribution of IL-1β towards persistent inflammation in chronic wounds and its role in impaired wound healing [15]. However, the effects of IL-1β signaling in the context of diabetic wound healing have not been studied so far. Therefore, in this study, we explored the role of IL-1β in diabetic wound closure using patient tissues and *ex vivo* fibroblast cultures and identified a novel mechanism behind delayed wound healing observed in patients with diabetes mellitus.

2. Methods

2.1. Clinical Specimens. All patients were recruited from the Department of Orthopedic Surgery, Shanghai Jiao Tong University Affiliated Sixth People's Hospital. Patients characterized for type 2 diabetes with chronic wounds located on the foot and nondiabetic patients (control group) with a leg wound were enrolled in our study. Patients presenting chronic wounds resulting from pressure ulcer, pyoderma gangrenosum, vasculitis, and other diseases that cause ischemia were excluded. Serum and wound tissue samples of nondiabetic ($n = 30$) and type 2 diabetic ($n = 30$) patients were collected. This study was approved by the Ethic Review Board of Shanghai Six People's Hospital affiliated to Shanghai Jiao Tong University (YS-2019-010) and was in accordance with the principles of the declaration of Helsinki as amended. Written informed consent was obtained from each participant.

2.2. Cell Culture. To culture fibroblasts *ex vivo*, human tissue specimens were cut into 1-3 mm^3 cubes, digested in 0.15% collagenase (Roche Applied Science, Indianapolis, IN, USA), and cultured in DMEM medium (Gibco, Gaithersburg, MD, USA) at 37°C for 3 h [16]. Single-cell suspensions were then filtered through nylon meshes and centrifuged at 1500 rpm for 5 min. Pellet containing fibroblasts was resuspended and seeded in 10 cm plates in fully supplemented DMEM containing 10% fetal bovine serum (Invitrogen, Carlsbad, CA, USA). Cells were cultured at 37°C and 5% CO_2. Confluent cells were passaged and subcultured at 1 : 3 ratio. Cells were harvested for analysis after the first passage.

2.3. Mouse Skin Wound Samples. Male C57BL/6J mice were purchased from the Model Animal Research Center of Nanjing University. Diabetic (db/db) mice were created by knocking out the gene coding for the leptin receptor. The mice were maintained under 12 h light/12 h dark cycles and have unrestricted access to food and water at a controlled temperature (25°C). The skin wound samples were collected as previously described. Briefly, 8-week-old mice were anesthetized using ether following which the hair of the back skin was removed with a hair clipper. Two circular full-thickness wounds were made on the skin with a 6 mm skin biopsy trephine (Kai Industries, Inc., Gifu, Japan). On day 7 postwounding, mice were euthanized by cervical dislocation and 2 mm peripheral skin from the wounded region was collected. The skin samples were immediately immersed in liquid nitrogen and stored at -80°C until further use. All animal experiments have been approved by the Animal Care and Use Committee of the Shanghai Jiao Tong University and guidelines on animal care and use according to the National Institute of Health (NIH, USA) guidelines were followed.

2.4. Quantitative Real-Time PCR. Total RNA from cells or tissues was extracted using TRIzol and was subsequently reverse transcribed by RevertAid First Strand cDNA Synthesis Kit. Quantitative real-time PCR was performed using SYBR Green PCR mix on an ABI Prism 7500HT (Applied Biosystems) with GAPDH as negative control. The primer pairs used were as follows: hIL-1β, ATGATGGCTTATTA CAGTGGCAA and GTCGGAGATTCGTAGCTGGA; hMMP2, TACAGGATCATTGGCTACACACC and GGTC ACATCGCTCCAGACT; hMMP9, GGGACGCAGACATC GTCATC and TCGTCATCGTCGAAATGGGC; hTIMP1, AGAGTGTCTGCGGATACTTCC and CCAACAGTGTA GGTCTTGGTG; hTIMP2, AAGCGGTCAGTGAGAAGGA AG and GGGGCCGTGTAGATAAACTCTAT; hGAPDH, AGCCACATCGCTCAGACAC and GCCCAATACGA CCAAATCC; mIL-1β, GCAACTGTTCCTGAACTCAACT and ATCTTTTGGGGTCCGTCAACT; mMMP2, CAAG TTCCCCGGCGATGTC and TTCTGGTCAAGGTCAC CTGTC; mMMP9, CTGGACAGCCAGACACTAAAG and CTCGCGGCAAGTCTTCAGAG; mTIMP1, GCAACT CGGACCTGGTCATAA and CGGCCCGTGATGAGAA ACT; mTIMP2, TCAGAGCCAAAGCAGTGAGC and GCCGTGTAGATAAACTCGATGTC; and mGAPDH, AGGTCGGTGTGAACGGATTTG and TGTAGACCATG TAGTTGAGGTCA.

2.5. Western Blotting. Tissues and cells were lysed with lysis buffer containing 50 mM Tris-HCl (pH 6.8), 2% sodium dodecyl sulfate, 10 mM dithiothreitol, 10% glycerol, 0.002% bromophenol blue, and protease inhibitor cocktail (Roche, Basel, Switzerland). Total protein quantification was performed using Pierce BCA Protein Assay Kit (ThermoFisher Scientific). Equal amounts of protein were loaded and separated by sodium dodecylsulfate (SDS)-polyacrylamide gel electrophoresis and transferred onto PVDF membranes (Millipore, Billerica, MA, USA). Membranes were blocked in 5% bovine serum albumin or nonfat milk and incubated with antibodies overnight at 4°C. The primary antibodies against IL-1β, MMP2, MMP9, TIMP1, TIMP2, collagenase I, collagenase III, p-p38 mitogen-activated protein kinase (MAPK), p-protein kinase B (AKT), AKT, p-phosphatidylinositol 3 kinase (PI3K), PI3K, and β-actin were purchased from Cell Signaling Technology (Danvers, MA, USA). After 3x washing with TBS-Tween 20, the membranes were incubated with secondary antibodies coupled to horseradish peroxidase for 1 hour at room temperature. Protein bands were visualized using chemiluminescence.

2.6. Cell Viability Assay. CCK8 assay was performed to analyze cell viability. Cells were seeded in 96-well plates in quintuplicates at a density of 1×104 cells/well and maintained in a humidified atmosphere of 5% CO_2 at 37°C. The plated cells were incubated with IL-1β at 5, 50, or 100 ng/mL concentration for different times. Cells were then treated with 10 μL/well CCK8 solution (Dojindo Molecular Technologies, Japan) for 2 hours. The OD450 in each well was determined by a microplate reader, reflecting the amount of total viable cells under each condition.

2.7. Migration Assay. A scrape wound assay was used to evaluate cell motility. Normal healthy fibroblasts or fibroblasts were seeded from diabetic patients in 6 cm dishes. Confluent cells were scraped using a sterilized 200 μL tip, and nonadherent cells were washed off with medium. The healthy
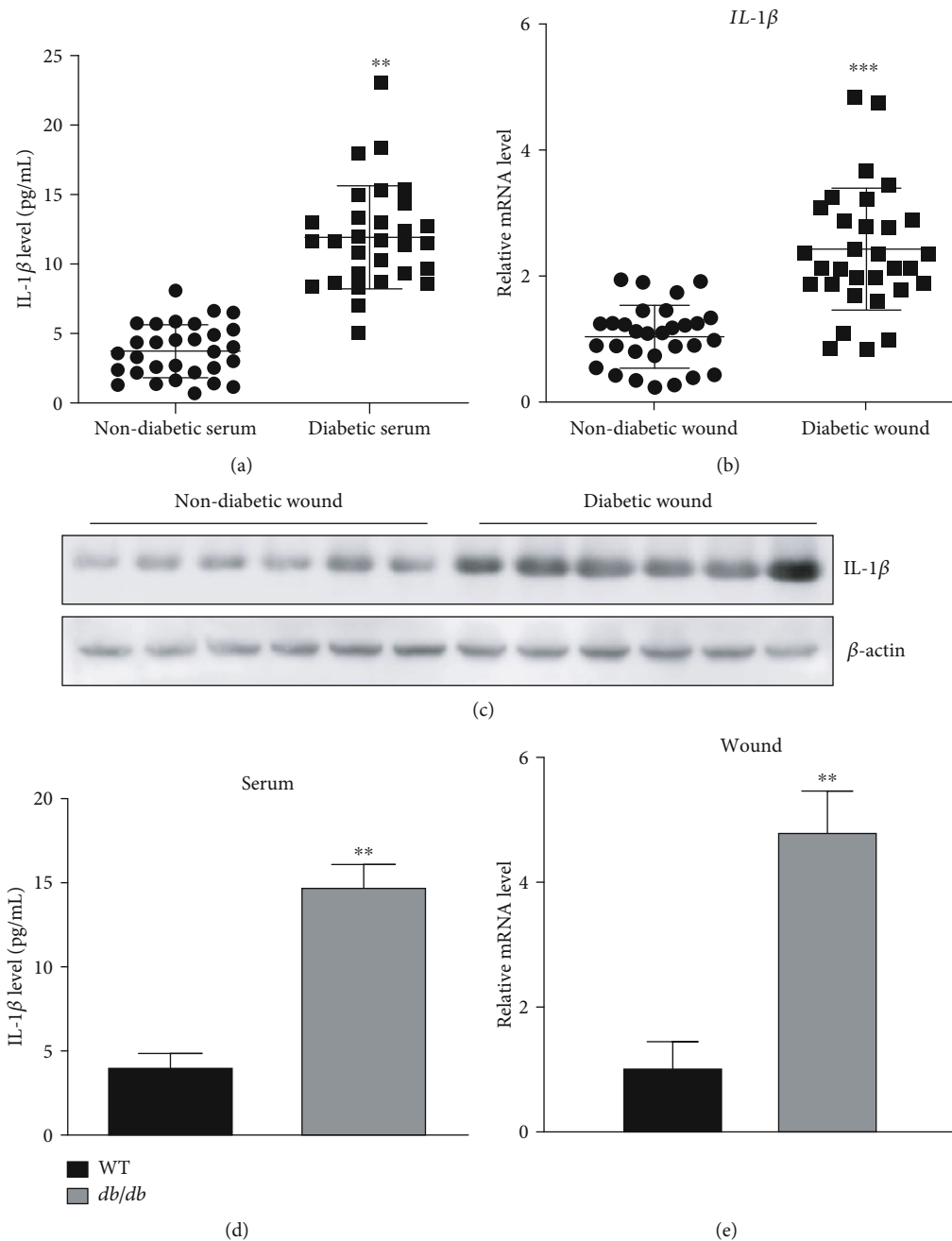
FIGURE 1: IL-1β levels were increased in diabetic wound tissues: (a) levels of IL-1β in the serum of patients as detected by ELISA; (b) mRNA levels of IL-1β in wound tissues as measured by qPCR; (c) protein levels of IL-1β in wound tissues; (d, e) IL-1β levels in serum and wound tissues in WT and db/db mice. $^{**}p < 0.01$; $^{***}p < 0.001$.

fibroblast cells were then treated with the indicated dose of IL-1β for 72 hours. Cells in the migrated fraction was photographed using a microscope, and the percentage of total area covered by the cells in each image was calculated using ImageJ (National Institutes of Health, USA). Three independent experiments were performed.

2.8. ELISA. Measurement of IL-1β in the serum from clinical samples or mice was performed using human or mouse IL-1β Quantikine ELISA Kit (R&D systems), respectively, according to manufacturer's instructions.

2.9. Statistical Analysis. Data was represented as mean ± standard deviation (SD) from at least three or more independent experiments. Statistical significance was calculated using Student's *t*-test or one-way ANOVA followed by Tukey's post hoc test. $p \leq 0.05$ was considered as statistically significant.

3. Results

3.1. IL-1β Levels Were Increased in the Wounds of Patients with Diabetes. To study the role of IL-1β in wound healing

(a)

(b)
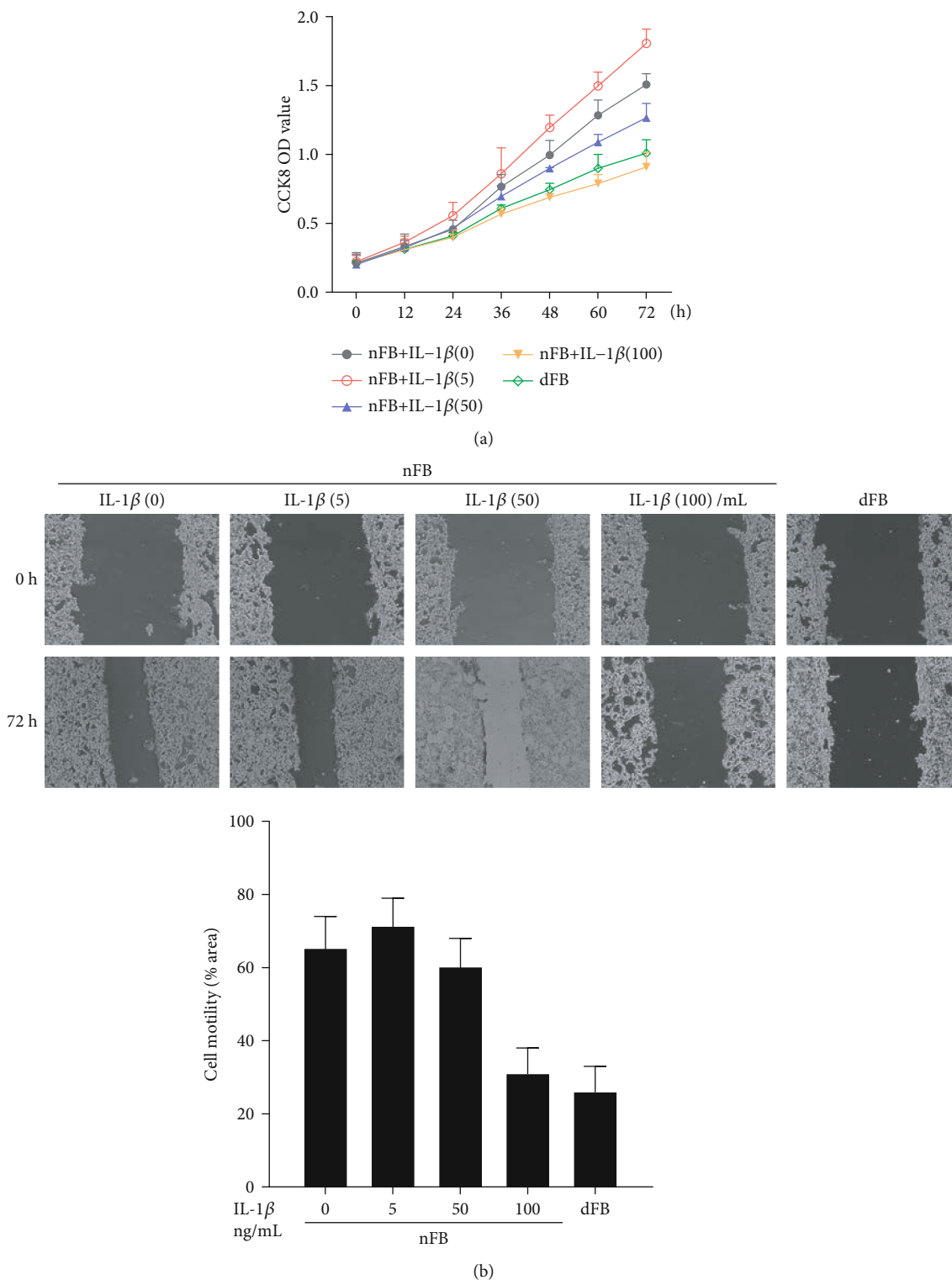
Figure 2: High dose of IL-1β inhibits proliferation and migration of fibroblasts *ex vivo*: (a) CCK8 assay indicating cell viability of normal (nFB) and diabetic fibroblasts (dFB) under different concentrations of IL-1β (0, 5, 50, 100 ng/mL); (b) cell proliferation of fibroblasts under different concentrations of IL-1β. Representative images and quantification are shown. $^{*}p < 0.05$.

in patients with diabetes, we collected serum and wound tissues from normal and diabetic individuals and performed ELISA/western blots to measure protein levels of IL-1β in the serum and tissues, respectively, and qPCR to measure IL-1β mRNA levels. We found that IL-1β was upregulated in the serum of diabetic patients (Figure 1(a)). Consistently, mRNA and protein levels were also increased in wound tissues of diabetic patients when compared to normal tissues
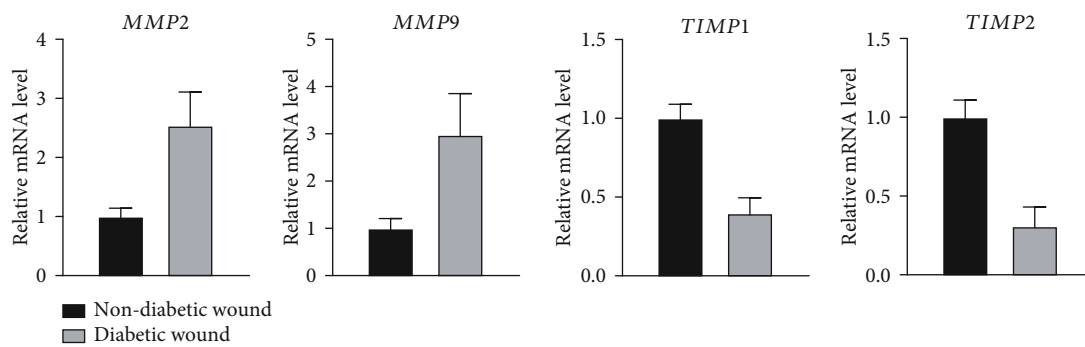
(a)
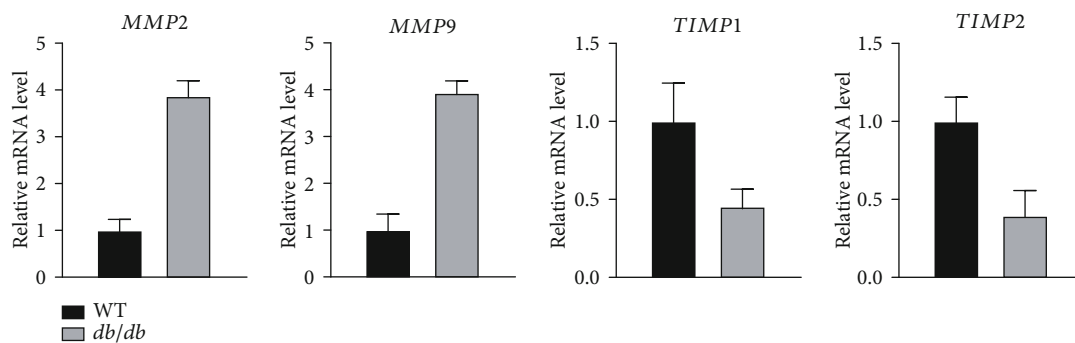
(b)
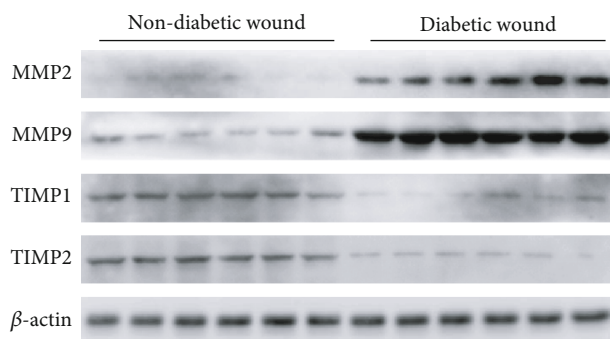
(c)

Figure 3: Continued.

(d)

(e)
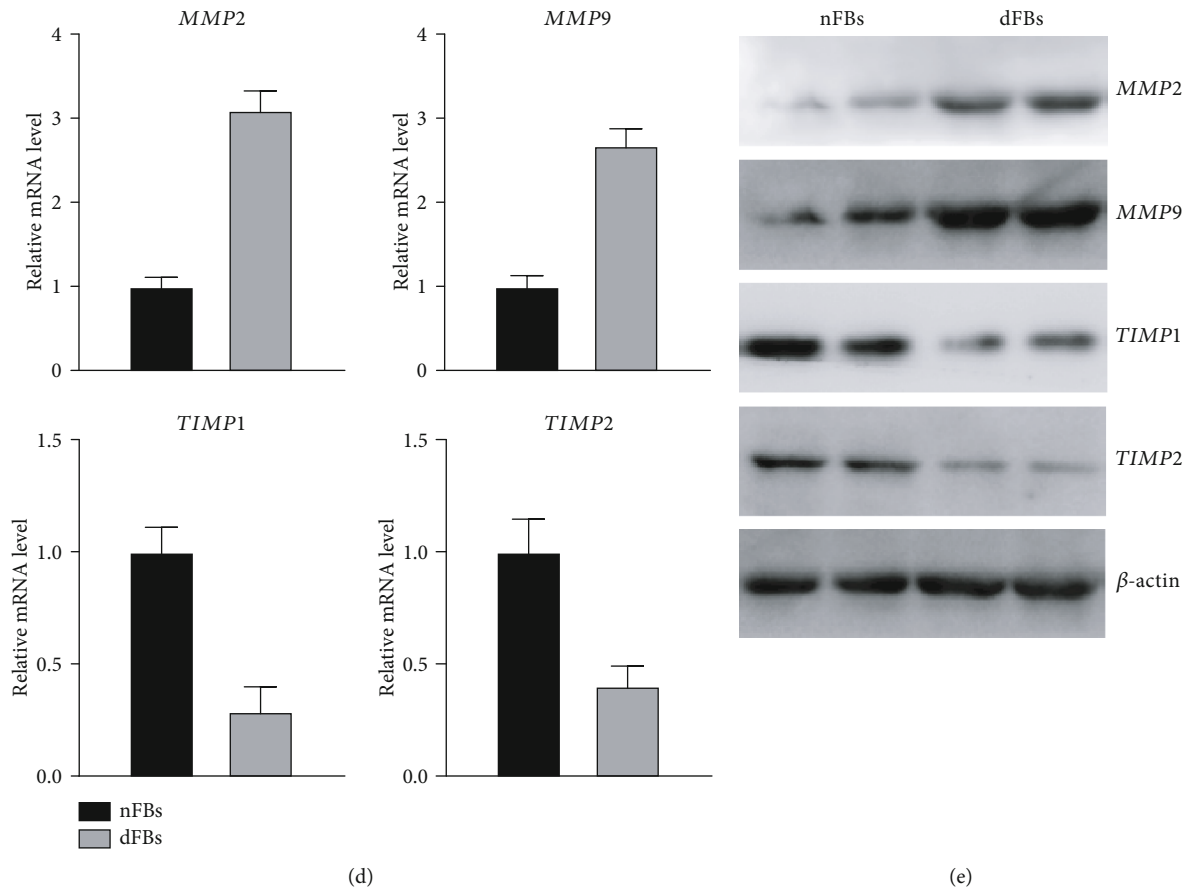
FIGURE 3: Diabetic wounds display elevated MMP expression and reduced TIMP expression: (a) mRNA levels of MMP2, MMP9, TIMP1, and TIMP2 in nondiabetic and diabetic wound tissues from patients evaluated by qPCR; (b) mRNA levels of MMP2, MMP9, TIMP1, and TIMP2 in control and db/db wound tissues from mice; (c) protein expression of MMP2, MMP9, TIMP1, and TIMP2 in nondiabetic and diabetic wounds evaluated by western blot; (d, e) mRNA quantification (d) and protein expression (e) in nFB and dFB samples. $^*p < 0.05$.

(Figures 1(b) and 1(c)). We then evaluated levels of IL-1β in wound tissues from db/db type 2 diabetic wound healing mouse model and observed that expression of IL-1β was significantly higher in the serum and wounds from diabetic mice when compared to normal mice (Figures 1(d) and 1(e)). Together, these results indicate that IL-1β is upregulated in wound tissues under diabetic conditions.

3.2. High Levels of IL-1β Inhibit Proliferation and Migration of Fibroblasts. We cultured primary fibroblasts from normal or diabetic wound tissues *ex vivo* and observed a decrease in cell proliferation in diabetic fibroblasts (dFB) when compared to normal fibroblasts (nFB) (Figure 2(a)). We then evaluated the effect of IL-1β on fibroblast proliferation and observed that low dose of IL-1β had no effect or promoted cell proliferation whereas a higher dose significantly inhibited proliferation of fibroblast (Figure 2(a)). Further, scrape wound assay was used to determined cell motility and we found that dFB displayed impaired migration capability when compared to nFB. The effect on migration was dependent on levels of IL-1β as we observed a decrease in cell migration with increasing concentrations of IL-1β (Figure 2(b)). Taken together, these results indicate that high

levels of IL-1β impair cell proliferation and migration in fibroblasts *ex vivo*.

3.3. Expression of MMPs Is Upregulated in Diabetic Wounds whereas TIMP Proteins Are Downregulated. As several studies showed that MMPs were potential predictive markers for impaired wound closure in diabetic foot ulcers [17], we next measured protein and mRNA levels of MMP-2, MMP-9, TIMP1, and TIMP2 in tissues and cultured fibroblasts from diabetic wound patients and compared them with the normal control group. We found that the mRNA expression of MMP2 and MMP9 was significantly upregulated in the wounds of diabetic patients while the expression of TIMP1 and TIMP2 that are inhibitors of MMP2 and MMP9, respectively, was significantly downregulated in diabetic wounds when compared to normal wounds (Figure 3(a)). We then evaluated TIMP1 and TIMP2 expression in wound tissues of db/db and control mice and observed a similar effect (Figure 3(b)). These results were further confirmed at the protein level by western blot using samples from the wounds of diabetic and nondiabetic patients. MMP2 and MMP9 protein expression was significantly higher in diabetic wound samples when compared to nondiabetic wounds, while
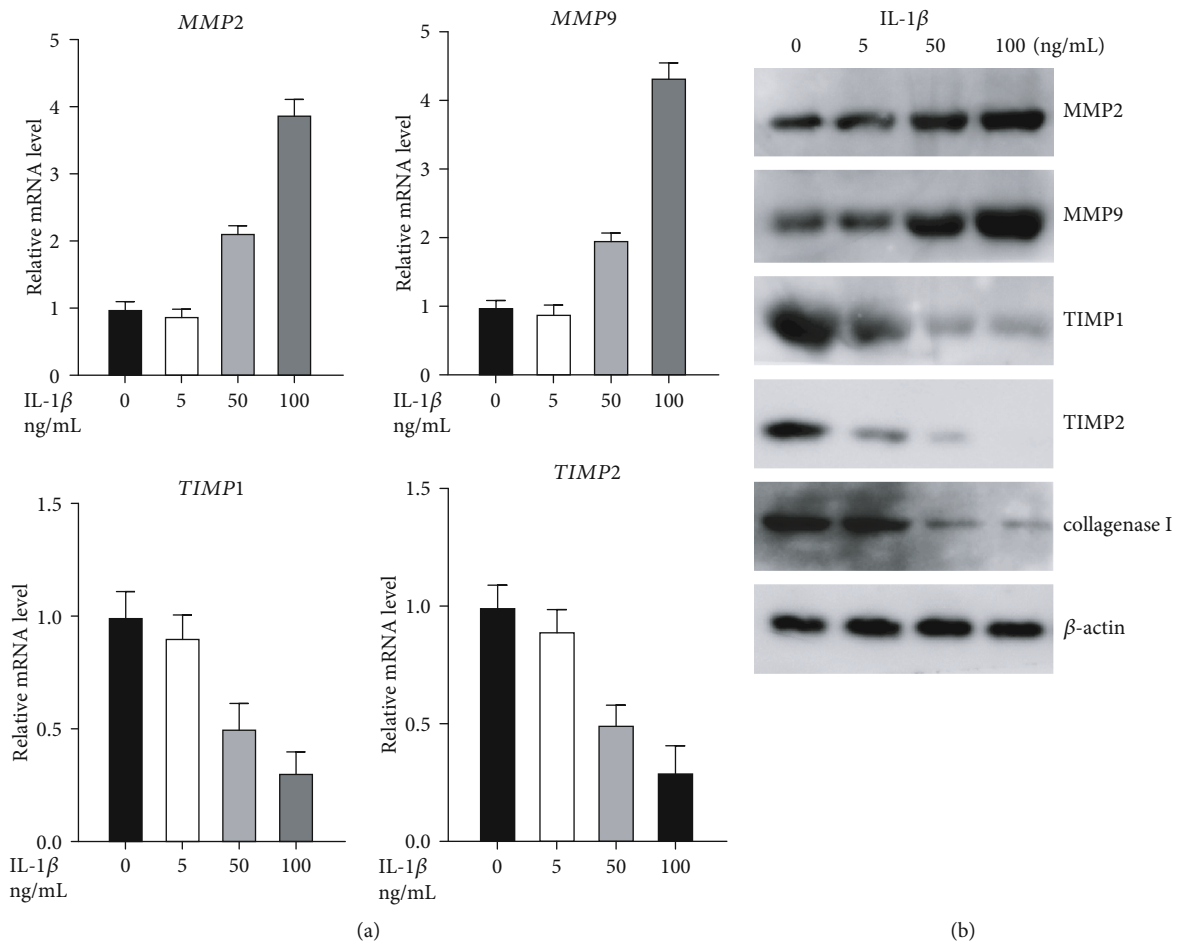
FIGURE 4: IL-1β induces MMP expression and inhibits TIMP expression *ex vivo*: (a, b) mRNA and protein levels of MMP2, MMP9, TIMP1, and TIMP2 in nFB at various doses of IL-1β. $^*p < 0.05$.

TIMP1 and TIMP2 expression levels were significantly lower in diabetic wound tissues (Figure 3(c)). We then validated these results in cultured fibroblasts and observed that both mRNA and protein levels of MMP2 and MMP9 were upregulated in dFBs while TIMP1 and TIMP2 expression was downregulated (Figures 3(d) and 3(e)). Taken together, our results indicate that diabetic conditions increase expression of MMP proteins in wound tissues while simultaneously downregulating expression of TIMP proteins.

3.4. IL-1β Induced Expression of MMPs and Downregulated Expression of TIMP Proteins Ex Vivo. We next evaluated the effects of IL-1β on the expression of MMPs and TIMPs in primary fibroblasts *ex vivo*. IL-1β was found to upregulate the expression of MMP2 and MMP9 in a dose-dependent manner as quantified by qPCR, while simultaneously inhibiting the expression of TIMP1 and TIMP2 (Figure 4(a)). We observed similar results when measuring protein expression by western blot. IL-1β inhibited the expression of collagenase I which facilitates wound healing along with TIMP1 and TIMP2 while simultaneously promoting the expression of MMP2 and MMP9 (Figure 4(b)). These results indicate that levels of MMP and TIMP proteins that are involved in the process of wound healing are directly regulated by IL-1β.

3.5. IL-1β Expression Regulates the Activation of p38 MAPK Pathway. We measured the effects of IL-1β treatment on the activation of p38 MAPK, PI3K, and AKT pathways in cultured fibroblasts. IL-1β treatment increased phosphorylation of p38 in a dose-dependent manner but not AKT and PI3K (Figure 5(a)). We next measured the expression levels of MMPs and TIMPs in the presence and absence of p38 MAPK inhibitor SB203580 (10 μM) and observed that treatment with an inhibitor reduced the effects of IL-1β on the expression of ECM remodeling proteins MMPs and TIMPs and collagenase (Figure 5(b)). Furthermore, inhibitor treatment also reduced the effect of IL-1β on cell proliferation (Figure 5(c)). Phosphorylated p38 expression was significantly higher in sections from diabetic wounds when compared to nondiabetic wound samples (Figure 5(d)). Together, these results indicate that IL-1β regulates the expression of ECM remodeling proteins in wound tissues via the p38 MAPK pathway in diabetes mellitus.

4. Discussion

In the present study, we confirmed the increase in levels of IL-1β in patients with type 2 diabetes mellitus that was also previously reported by several studies [18, 19]. Current

(a)

(b)

(c)

(d)
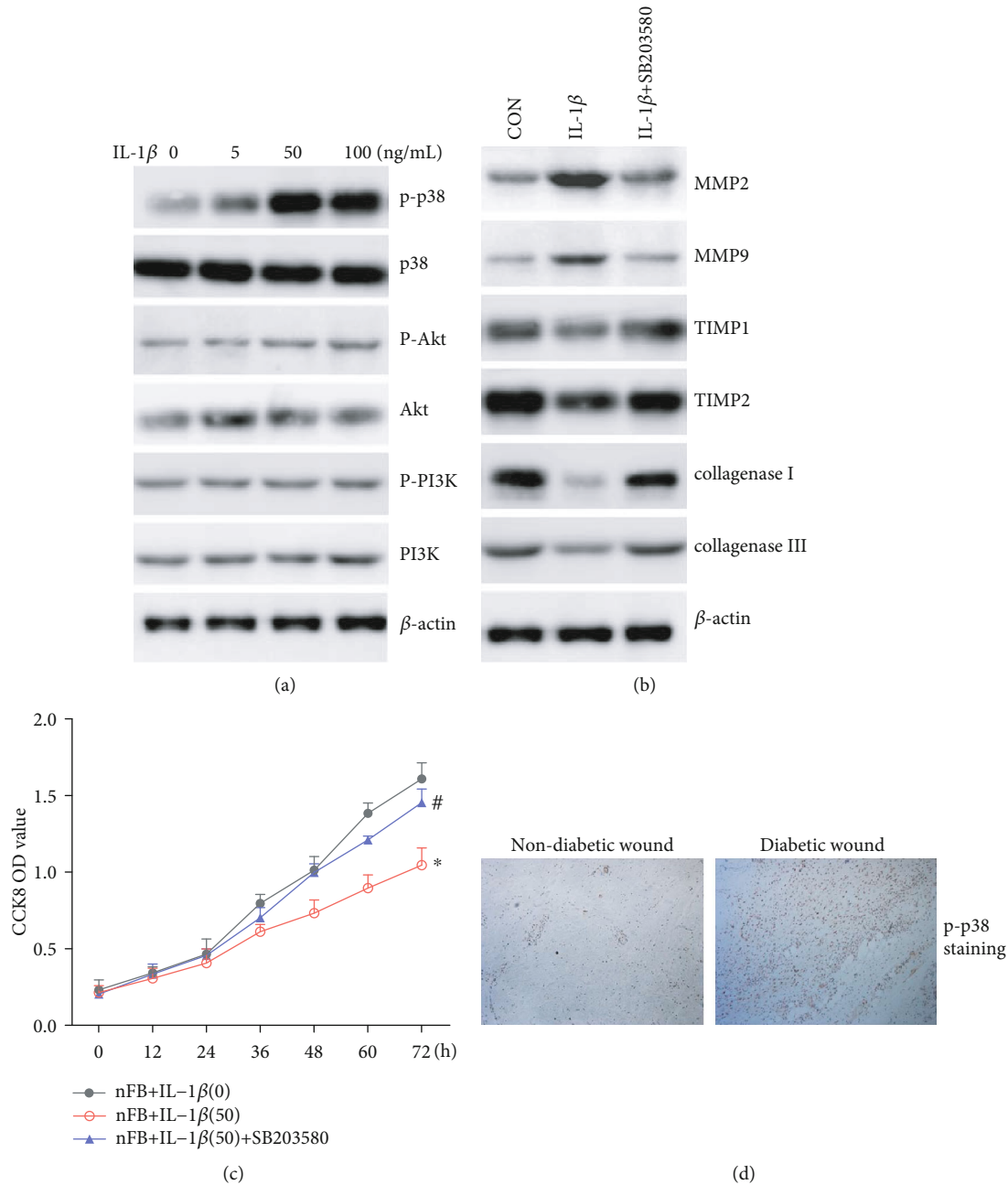
FIGURE 5: IL-1β activates the p38 MAPK pathway to mediate its effects in wound healing. (a) Activation of p38 MAPK, PI3K, and AKT was measured upon IL-1β treatment. (b) p38 MAPK inhibitor SB203580 (10 μM) was used to treat nFB. Protein levels of MMP2, MMP9, TIMP1, and TIMP2 were measured. (c) p38 MAPK inhibitor SB203580 (10 μM) was used to treat nFB. Cell proliferation of fibroblasts was detected. (d) p-p38 MAPK staining in diabetic and nondiabetic wounds.

theories regarding the pathophysiology of diabetes conceptualize the disease as a proinflammatory state characterized, among other things, by elevated levels of IL-1β. Blockade of the effects of IL-1β is therefore a promising focus of study in diabetes therapeutics [20]. Toll-like receptors and the Nod-like receptor protein-3 (NLRP3) inflammasome, as well as interleukin-1β, all appear to participate in the pathogenesis of diabetes [21]. Several studies have highlighted the importance of IL-1 in the pathogenesis of type 2 diabetes and identified it as a promising therapeutic strategy [22–25]. Although Mandrup-Poulsen and the AIDA study group

(2013) reported that IL-1 inhibitor treatment is not effective against type 1 diabetes [26], its outcomes in mitigating type 2 diabetes remain to be evaluated. In order to pursue this approach as an efficient treatment strategy, the molecular mechanisms underlying the effects of IL-1 in type 2 diabetes is necessary.

The role of IL-1β in diabetic wound healing has been described previously. Mirza et al. reported that IL-1β plays a key role in sustaining the proinflammatory macrophage phenotype and in impairing the healing of diabetic wounds [15]. Treatment with an inhibitor of IL-1 receptor reversed

the impaired wound healing process in a diabetic mouse model [27]; however, the mechanism behind this effect was not elucidated. We observed that elevated levels of IL-1β in diabetic wound tissues triggers the secretion of MMPs and inhibits expression of TIMP proteins to interfere with ECM remodeling and wound closure. In the process of pulmonary fibrosis, IL-1β stimulates the proliferation of fibroblasts and the production of type I and III collagen [28]. Furuyama et al. described that IL-1β induces the secretion of MMP-2 and MMP-9 in fibroblasts, thereby inhibiting the formation of basement membrane [29], which is in accordance with our results. These findings indicate that IL-1β regulates the formation and degradation of ECM in fibroblasts; however, the discrepancy between the studies may be due to the levels of IL-1β used as we also observed an inhibitory effect on fibroblast proliferation and migration only under high concentrations, as observed in diabetic patient samples, whereas low concentrations of IL-1β promoted cell proliferation.

Remodeling of the ECM is a primary requirement for wound closure [30] and MMPs are an important family of cell migration-related proteins that can degrade different components of the ECM [31]. Our results showed that both mRNA and protein levels of MMPs were higher in diabetic wounds than those in the control group, while levels of TIMP were lower. These results suggest that diabetic wounds are characterized by greater breakdown of ECM, a phenomenon that delays wound healing. It is proven by many studies that levels of MMPs are higher in the exudates of chronic wounds than in those of acute wounds, as in diabetic foot ulcers [32]. Addition of IL-1β stimulated the expression of MMPs and inhibited the production of TIMPs and collagenase suggesting that IL-1β promotes ECM degradation and delays the process of wound healing in diabetes.

We also observed that the action of IL-1β may at least in part be mediated by the p38 MAPK pathway. It is well known that p38 MAPK is capable of regulating a variety of cellular responses to cytokines and stress, including IL-1β [33]. p38 was found to promote the invasion and migration of gastric adenocarcinoma cells by increasing the levels of MMPs [34]. The addition of IL-1β to cultured fibroblasts resulted in increased phosphorylation of p38 in a dose-dependent manner whereas it showed no effect in AKT and PI3K. Phosphorylated p38, the activated form of p38, was also significantly higher in sections from diabetic wound tissues than in nondiabetic wounds and treatment with p38 MAPK inhibitor SB203580 reversed the effects of IL-1β on ECM remodeling protein expression.

5. Conclusions

Taken together, our study suggests that IL-1β mediates delayed wound healing in diabetic patients by altering levels of ECM remodeling proteins through activation of the p38 MAPK pathway thereby impairing cell proliferation and migration. It also identifies IL-1β as a potential therapeutic target to treat delayed wound closure in type 2 diabetic patients.

Abbreviations

MMP: Matrix metalloproteinase
TIMP: Tissue inhibitor of metalloproteinase
NLRP3: Nod-like receptor protein-3
ECM: Extracellular matrix
MAPK: Mitogen-activated protein kinase
AKT: Protein kinase B
PI3K: Phosphatidylinositol 3 kinase.

Data Availability

The data used to support the findings of this study are included within the article, which are available from the corresponding author upon request.

Ethical Approval

This study was approved by the Ethic Review Board of Shanghai Sixth People's Hospital affiliated to Shanghai Jiao Tong University.

Conflicts of Interest

All the authors declare that they have no conflict of interest.

Authors' Contributions

Jiezhi Dai was responsible for investigation and writing the original draft. Junjie Shen was responsible for the methodology. Yimin Chai was responsible for writing, review, and editing. Hua Chen was responsible for the conceptualization, writing, review, and editing. Jiezhi Dai and Junjie Shen contributed equally as first authors.

Acknowledgments

References

[1] L. Guariguata, D. R. Whiting, I. Hambleton, J. Beagley, U. Linnenkamp, and J. E. Shaw, "Global estimates of diabetes prevalence for 2013 and projections for 2035," *Diabetes Research and Clinical Practice*, vol. 103, no. 2, pp. 137–149, 2014.

[2] K. Ogurtsova, J. D. da Rocha Fernandes, Y. Huang et al., "IDF Diabetes Atlas: global estimates for the prevalence of diabetes for 2015 and 2040," *Diabetes Research and Clinical Practice*, vol. 128, pp. 40–50, 2017.

[3] J. Yin, A. P. Kong, and J. C. Chan, "Prevention and care programs addressing the growing prevalence of diabetes in China," *Current Diabetes Reports*, vol. 16, no. 12, p. 130, 2016.

[4] A. J. Boulton, L. Vileikyte, G. Ragnarson-Tennvall, and J. Apelqvist, "The global burden of diabetic foot disease," *Lancet*, vol. 366, no. 9498, pp. 1719–1724, 2005.

[5] A. W. Seifert, J. R. Monaghan, S. R. Voss, and M. Maden, "Skin regeneration in adult axolotls: a blueprint for scar-free healing in vertebrates," *PLoS One*, vol. 7, no. 4, article e32875, 2012.

[6] R. Richardson, K. Slanchev, C. Kraus, P. Knyphausen, S. Eming, and M. Hammerschmidt, "Adult zebrafish as a model system for cutaneous wound-healing research," *The Journal of Investigative Dermatology*, vol. 133, no. 6, pp. 1655–1665, 2013.

[7] M. Takeo, W. Lee, and M. Ito, "Wound healing and skin regeneration," *Cold Spring Harbor Perspectives in Medicine*, vol. 5, no. 1, 2015.

[8] S. Barrientos, O. Stojadinovic, M. S. Golinko, H. Brem, and M. Tomic-Canic, "Growth factors and cytokines in wound healing," *Wound Repair and Regeneration*, vol. 16, no. 5, pp. 585–601, 2008.

[9] P. K. Young and F. Grinnell, "Metalloproteinase activation cascade after burn injury: a longitudinal analysis of the human wound environment," *The Journal of Investigative Dermatology*, vol. 103, no. 5, pp. 660–664, 1994.

[10] M. A. Moses, M. Marikovsky, J. W. Harper et al., "Temporal study of the activity of matrix metalloproteinases and their endogenous inhibitors during wound healing," *Journal of Cellular Biochemistry*, vol. 60, no. 3, pp. 379–386, 1996.

[11] K. Brew, D. Dinakarpandian, and H. Nagase, "Tissue inhibitors of metalloproteinases: evolution, structure and function[1]," *Biochimica et Biophysica Acta*, vol. 1477, no. 1-2, pp. 267–283, 2000.

[12] M. Vaalamo, T. Leivo, and U. Saarialho-Kere, "Differential expression of tissue inhibitors of metalloproteinases (TIMP-1, -2, -3, and -4) in normal and aberrant wound healing," *Human Pathology*, vol. 30, no. 7, pp. 795–802, 1999.

[13] C. Soo, W. W. Shaw, X. Zhang, M. T. Longaker, E. W. Howard, and K. Ting, "Differential expression of matrix metalloproteinases and their tissue-derived inhibitors in cutaneous wound repair," *Plastic and Reconstructive Surgery*, vol. 105, no. 2, pp. 638–647, 2000.

[14] X. Zhang, J. Dai, L. Li, H. Chen, and Y. Chai, "NLRP3 inflammasome expression and signaling in human diabetic wounds and in high glucose induced macrophages," *Journal Diabetes Research*, vol. 2017, article 5281358, pp. 1–7, 2017.

[15] R. E. Mirza, M. M. Fang, W. J. Ennis, and T. J. Koh, "Blocking interleukin-1 induces a healing-associated wound macrophage phenotype and improves healing in type 2 diabetes," *Diabetes*, vol. 62, no. 7, pp. 2579–2587, 2013.

[16] Z. Jiang, Q. Yu, L. Xia et al., "Growth differentiation factor-9 promotes fibroblast proliferation and migration in keloids through the Smad2/3 pathway," *Cellular Physiology and Biochemistry*, vol. 40, no. 1-2, pp. 207–218, 2016.

[17] J. I. Jones, T. T. Nguyen, Z. Peng, and M. Chang, "Targeting MMP-9 in diabetic foot ulcers," *Pharmaceuticals (Basel)*, vol. 12, no. 2, p. 79, 2019.

[18] B. Fève and J. P. Bastard, "The role of interleukins in insulin resistance and type 2 diabetes mellitus," *Nature Reviews. Endocrinology*, vol. 5, no. 6, pp. 305–311, 2009.

[19] M. Böni-Schnetzler, J. Thorne, G. Parnaud et al., "Increased interleukin (IL)-1beta messenger ribonucleic acid expression in beta-cells of individuals with type 2 diabetes and regulation of IL-1beta in human islets by glucose and autostimulation," *The Journal of Clinical Endocrinology and Metabolism*, vol. 93, no. 10, pp. 4065–4074, 2008.

[20] K. Maedler, G. Dharmadhikari, D. M. Schumann, and J. Størling, "Interleukin-targeted therapy for metabolic syndrome and type 2 diabetes," *Handbook of Experimental Pharmacology*, vol. 203, pp. 257–278, 2011.

[21] E. K. Grishman, P. C. White, and R. C. Savani, "Toll-like receptors, the NLRP3 inflammasome, and interleukin-1β in the development and progression of type 1 diabetes," *Pediatric Research*, vol. 71, no. 6, pp. 626–632, 2012.

[22] M. Banerjee and M. Saxena, "Interleukin-1 (IL-1) family of cytokines: role in type 2 diabetes," *Clinica Chimica Acta*, vol. 413, no. 15-16, pp. 1163–1170, 2012.

[23] M. S. Akash, Q. Shen, K. Rehman, and S. Chen, "Interleukin-1 receptor antagonist: a new therapy for type 2 diabetes mellitus," *Journal of Pharmaceutical Sciences*, vol. 101, no. 5, pp. 1647–1658, 2012.

[24] T. Mandrup-Poulsen, L. Pickersgill, and M. Y. Donath, "Blockade of interleukin 1 in type 1 diabetes mellitus," *Nature Reviews. Endocrinology*, vol. 6, no. 3, pp. 158–166, 2010.

[25] T. Mandrup-Poulsen, "Interleukin-1 antagonists and other cytokine blockade strategies for type 1 diabetes," *The Review of Diabetic Studies*, vol. 9, no. 4, pp. 338–347, 2012.

[26] T. Mandrup-Poulsen, "Interleukin-1 antagonists for diabetes," *Expert Opinion on Investigational Drugs*, vol. 22, no. 8, pp. 965–979, 2013.

[27] D. P. Perrault, A. Bramos, X. Xu, S. Shi, and A. K. Wong, "Local administration of interleukin-1 receptor antagonist improves diabetic wound healing," *Annals of Plastic Surgery*, vol. 80, no. 5S, pp. S317–S321, 2018.

[28] J. Vilcek, V. J. Palombella, D. Henriksen-DeStefano et al., "Fibroblast growth enhancing activity of tumor necrosis factor and its relationship to other polypeptide growth factors," *The Journal of Experimental Medicine*, vol. 163, no. 3, pp. 632–643, 1986.

[29] A. Furuyama, T. Hosokawa, and K. Mochitate, "Interleukin-1beta and tumor necrosis factor-alpha have opposite effects on fibroblasts and epithelial cells during basement membrane formation," *Matrix Biology*, vol. 27, no. 5, pp. 429–440, 2008.

[30] N. S. Greaves, K. J. Ashcroft, M. Baguneid, and A. Bayat, "Current understanding of molecular and cellular mechanisms in fibroplasia and angiogenesis during acute wound healing," *Journal of Dermatological Science*, vol. 72, no. 3, pp. 206–217, 2013.

[31] X. WU, L. YANG, Z. ZHENG et al., "Src promotes cutaneous wound healing by regulating MMP-2 through the ERK pathway," *International Journal of Molecular Medicine*, vol. 37, no. 3, pp. 639–648, 2016.

[32] R. Lobmann, A. Ambrosch, G. Schultz, K. Waldmann, S. Schiweck, and H. Lehnert, "Expression of matrix-metalloproteinases and their inhibitors in the wounds of diabetic and non-diabetic patients," *Diabetologia*, vol. 45, no. 7, pp. 1011–1016, 2002.

[33] Y. T. Yeung, N. S. Bryce, S. Adams et al., "P 38 MAPK inhibitors attenuate pro-inflammatory cytokine production and the invasiveness of human U251 glioblastoma cells," *Journal of Neuro-Oncology*, vol. 109, no. 1, pp. 35–44, 2012.

[34] Q. Huang, F. Lan, X. Wang et al., "IL-1β-induced activation of p38 promotes metastasis in gastric adenocarcinoma via upregulation of AP-1/c-fos, MMP2 and MMP9," *Molecular Cancer*, vol. 13, no. 1, pp. 18–4598, 2014.

Research Article

Agnuside Alleviates Synovitis and Fibrosis in Knee Osteoarthritis through the Inhibition of HIF-1α and NLRP3 Inflammasome

Li Zhang,[1,2] **Xiaochen Li,**[1,2] **Haosheng Zhang,**[1,2] **Zhengquan Huang** ![ORCID],[1,3] **Nongshan Zhang,**[1,3] **Li Zhang,**[1,3] **Runlin Xing,**[1,3] **and Peimin Wang** ![ORCID][1,3,4]

[1]*The Affiliated Hospital of Nanjing University of Chinese Medicine, Department of Orthopedics, Nanjing 210029, China*
[2]*Key Laboratory for Metabolic Diseases in Chinese Medicine, First College of Clinical Medicine, Nanjing University of Chinese Medicine, Nanjing 210023, China*
[3]*Jiangsu Province Hospital of Chinese Medicine, Nanjing, Jiangsu 210029, China*
[4]*Affiliated Hospital of Nanjing University of Chinese Medicine, Hanzhong Road 155, Nanjing, Jiangsu Province, China*

Correspondence should be addressed to Peimin Wang; drwpm@163.com

Increasing evidence has shown that NLRP3 inflammasome activation participates in chronic aseptic inflammation and is related to tissue fibrosis. Our last study also revealed the vital role of NLRP3 inflammasome, highly associated with tissue hypoxia, in the onset and development of knee osteoarthritis (KOA). In this study, we tried to find a possible benign intervention for that pathological process. Agnuside (AGN), a nontoxic, natural small molecule isolated from the extract of *Vitex negundo L.* (Verbenaceae), has been demonstrated to have antioxidation, anti-inflammatory, analgesia, and many other properties as an iridoid glycoside, although its specific target is still unclear. Therefore, we established MIA-induced KOA model rats and investigated the effects of AGN oral gavage on oxygen-containing state, NLRP3 inflammasome, synovitis, and fibrosis in KOA. Pimonidazole staining and HIF-1α immunohistochemical assay both showed that AGN at the oral dose of 6.25 mg/kg can effectively relieve local hypoxia in synovial tissue. Besides, we observed a decrease of HIF-1α, caspase-1, ASC, and NLRP3 after AGN intervention, both in the mRNA and protein levels. In addition, rats treated with the AGN showed less inflammatory reaction and fibrosis, not only in the expression of NLRP3, inflammasome downstream factors IL-1β and IL-18, and fibrosis markers TGF-β, TIMP1, and VEGF but also in the observation of HE staining, anatomical characteristics, Sirius Red staining, and type I collagen immunohistochemistry. Subsequently, we established LPS-induced models of fibroblast-like synoviocytes (FLSs) mimicking the inflammatory environment of KOA and activating NLRP3 inflammasome. FLSs treated with AGN (3 μM) resulted in a downregulation of HIF-1α and the components required for NLRP3 inflammasome activation. Meanwhile, the content of proinflammatory factors IL-1β and IL-18 in FLS supernatant was also reduced by AGN. In addition, both mRNA and protein levels of the fibrotic markers were significantly decreased after AGN management. To conclude, this study demonstrates that AGN alleviates synovitis and fibrosis in experimental KOA through the inhibition of HIF-1α accumulation and NLRP3 inflammasome activation. Additionally, not only does it reveal some novel targets for anti-inflammatory and antioxidant effects of AGN but also announces its potential value in treating KOA in humans.

1. Introduction

Chronic low-grade inflammation in synovial tissue is a major driver of the ongoing joint degeneration in knee osteoarthritis (KOA) [1]. Under this inflammatory condition, KOA synovium occurs with pathological changes such as synovitis and fibrosis, highly associated with the clinical symptoms of pain, joint swelling, and stiffness, ultimately leading to disability [2]. Moreover, synovium damage may increase oxygen consumption, setting the tissue into a state of local

hypoxia, which has been extensively studied in arthritis disorders, not just KOA [3]. Subsequently, hypoxia-inducible transcription factor-1α (HIF-1α) accumulation triggers cellular responses to adapt to the anoxia environment, thus further exacerbating the development of synovitis and fibrosis [4]. In our last study, the correlation between HIF-1α upregulation and the nod-like receptor protein (NLRP3) inflammasome activation during KOA was investigated in vivo and in vitro. We also revealed that increased HIF-1α in KOA aggravates synovitis and fibrosis via NLRP3 activation [5].

The NLRP3 inflammasome is considered the most characteristic of NLR family, which contains NLR protein 3, an apoptosis-associated speck-like protein containing a caspase recruitment domain (ASC), and pro-caspase-1 [6]. The assembly and activation of the NLRP3 inflammasome will lead to an inflammatory cascade response based on the maturation and secretion of IL-1β, IL-18, HMGB1, and even to cell pyroptosis [7]. Two steps are generally considered to be required to complete this process, the NF-κB signaling pathway activation under inflammatory stimuli and pro-caspase-1 cleaved (to cleaved caspase-1 p10 and p20) via pathogen-associated molecular patterns (PAMPs) and damage-associated molecular patterns (DAMPs). Notably, these "steps" also play a vital role in the pathology of KOA. Besides, increasing evidence has shown that NLRP3 activation in different tissues (such as the liver, renal, and airway) participates in chronic aseptic inflammation and can be related to tissue fibrosis [8–10]. Therefore, how to treat chronic inflammation via the intervention of NLRP3 inflammasome becomes a hotspot.

Synovial fibrosis, another important aspect of KOA synovial lesions, has attracted increasing attention in recent years. Its main pathological changes include extracellular matrix (ECM) accumulation and angiogenesis [11]. Numerous studies have confirmed the collagen deposition effect of transforming growth factor-β (TGF-β), while the collagen degradation inhibition is mainly due to the tissue inhibitor of metalloproteinase 1 (TIMP1) [12, 13]. They both are crucial in regulating the ECM homeostasis. Previous studies also made detailed observations of angiogenesis in KOA synovial fibrosis, which may have highly similar pannus to rheumatoid arthritis under magnetic resonance imaging, and such pathological process is highly associated with vascular endothelial growth factor (VEGF) [14, 15]. Indeed, synovial fibrosis may largely be irreversible; therefore, antifibrotic therapy aimed at slowing down the fibrosis process is of great value in clinical application in KOA.

In the long-term practice of orthopedic treatment, we found "Sanse Powder," an external application, of traditional Chinese medicine, had a good clinical effect on treating KOA [16]. Subsequent studies explored the pharmaceutical components of "Sanse Powder" using ultraperformance liquid chromatography and identified agnuside (AGN), a nontoxic, natural small molecule isolated from the extract of *Vitex negundo L.* (Verbenaceae), as a part of medicinal effective ingredients [17]. Meanwhile, accumulating evidence has demonstrated the antioxidation, anti-inflammatory, analgesia, and many other properties of AGN as an iridoid glyco-

side [18–20]. Nevertheless, the medicinal effects of AGN evaluated in existing studies are still very limited, nor are the targets of AGN's efficacy clear.

In summary, KOA shows a combination of oxygen deficit and a state of low-grade inflammation, such pathological features are reflected in synovitis and fibrosis mediated by HIF-1α accumulation and NLRP3 activation. By targeting HIF-1α/NLRP3, AGN may have exerted antioxidation and anti-inflammatory effects. Accordingly, we hypothesized that AGN should alleviate synovitis and fibrosis in KOA through the inhibition of HIF-1α and NLRP3 inflammasomes.

2. Materials and Methods

2.1. In Vivo Animal Experimental Design. Twenty-four 2-month-old SD male rats, weight ranging from 210 g to 250 g (provided by Beijing Vital River Laboratory Animal Technology Co., Ltd.), were used. Animals were housed in a specific pathogen-free, laminar-flow housing apparatus under controlled temperature, humidity, and 12 h light/dark regimen and maintained on a standard rodent pellet diet. All animal protocols were approved by the Animal Care and Use Committee of the Nanjing University of Chinese Medicine. All experiments were conducted in accordance with the National Institutes of Health Guidelines for the Care and Use of Laboratory Animals. After one week of adaptive feeding, the first day of the experiment was recorded as Day 1.

Rats were randomly assigned to three groups: normal, KOA, and KOA+AGN, with eight rats in each group. On Day 1, the KOA model was constructed by inducing by intra-articular injection of 1 mg monosodium iodoacetate (MIA) as described previously, on both knees. 14 days after surgery (Day 14), the KOA model was successfully established, and drug administration began. 6.25 mg of AGN (Yuanye Bio-Technology Co., Ltd., Shanghai, China; HPLC > 98%) was prepared as suspension in 0.5% *w/v* sodium carboxymethyl cellulose in 10 ml sterilized physiologic saline. The KOA+AGN group received an oral dose (1 ml/100 g body weight/1 day) by oral gavage, while the other two groups received an equal volume of sodium carboxymethyl cellulose solution. After 21 days of AGN administration (Day 35), all rats were anesthetized with Nembutal, then abdominal aortic serum and synovial tissues were collected. The dosage, concentration, and intervention time of AGN are all referred to the previous study [19, 20].

2.2. Histological Analysis. Synovial tissues were fixed in 10% neutral formalin after rats were executed, embedded in paraffin, and cut into slices for routine staining. We followed Kenn's criteria in scoring and analyzing sections to evaluate synovitis [21].

Sirius Red staining was carried out according to the instructions of Sirius Red Stain kit (Beyotime Biotechnology, Shanghai, China). Sections were mounted and viewed under a Leica DMI3000B microscope (Leica, Germany), with the use of bright fields.

2.3. Immunohistochemical Assay. Immunohistochemistry stainings were performed to observe the expression of HIF-

1α and type I collagen in synovial tissue. We followed the methods of Peimin Wang et al. [22]. Briefly, sections were incubated in antigen retrieval buffer to unmask the antigen after a standard deparaffinization and rehydration process. Sections were treated with 3% hydrogen peroxide for 10 min. After that, the sections were permeabilized with 0.1% Triton X-100 in PBS for 5 min at room temperature, blocked with 1% BSA at room temperature for 1 h, and then incubated with primary antibodies (in 1% BSA, 0.1% Triton X-100) at 4°C overnight. For secondary reactions, species-matched HRP-labelled secondary antibody was used (1 : 500 in 1% BSA, 1 h) at 37°C. DAB was used as chromogen, and hematoxylin was used to counterstain. High-quality images were captured in six fields per sample, and semiquantitative analysis was measured by determining percentage of positive areas with ImageJ.

2.4. Pimonidazole Staining and Immunofluorescence. To investigate synovium tissue hypoxia, rats were injected with pimonidazole HCl (Hypoxyprobe™-1 Plus Kit, Burlington, MA, USA) at a dosage of 60 mg/kg for 45 min prior to sacrifice as previously described [4]. Subsequent immunofluorescence staining followed the kit instructions. The image was observed by inverted fluorescence microscope (Leica DMI3000B, Germany).

2.5. Cell Preparation and Treatment. Primary rat fibroblast-like synoviocytes (FLSs) were obtained from additional normal rats. In brief, synovial tissues were washed for 2-3 times with phosphate-buffered saline (PBS) and then minced into pieces of 2-3 mm^2, digested in 0.1% collagenase type II (Sigma, St. Louis, MO, USA) for 30 min. Following cell dissociation, the samples were filtered through a cell strainer. After dissociation, fibroblasts were pelleted by centrifugation at 1500 rpm for 4 min and cultured in DMEM supplemented with 10% fetal bovine serum (FBS; Gibco, Thermo Fisher Scientific, Waltham, MA, USA) and antibiotics (100 U/ml penicillin, 100 μg/ml streptomycin; Invitrogen, CA, USA). Cells were identified as our previous study [23]. Passages 3-6 of the synovial fibroblasts were used for the experiments.

Lipopolysaccharide (LPS), obtained from Sigma-Aldrich (St Louis, MO, USA), was used to simulate the inflammatory environment of KOA and activate the NLRP3 inflammasome. FLSs were stimulated with LPS (10 μg/ml) in DMEM for 6 h as the KOA group or exposed to DMEM with the same volume of PBS served as the normal group. The LPS +AGN group was treated with AGN (3 μM) for 24 h after the challenge of LPS, while the remaining groups were treated with PBS. The concentration and intervention time of AGN are all referred to the previous study [19, 20].

2.6. Caspase-1 Activity Analysis. After the treatment of AGN and/or LPS, FLSs were harvested and used to detect caspase-1 activity via Caspase-1 Activity Assay Kit (Beyotime Biotechnology, Shanghai, China) according to the manufacturer's instructions. The absorbance of the samples was measured at 405 nm using a microplate reader (PerkinElmer EnSpire, USA). All samples were quantified following comparison to

the normal group and calculated the relative changes of caspase-1 activity.

2.7. ELISA Assay. IL-1β and IL-18 levels in the rat serum and culture media were determined using a commercially available rat IL-1β and IL-18 enzyme-linked immunosorbent assay (ELISA) kit (Nanjing Jin Yibai Biological Technology Co. Ltd., Nanjing, China) according to the manufacturer's instructions.

2.8. Western Blotting. Briefly, synovial tissues or FLSs were mixed with RIPA lysate and grinded for 10-15 min, respectively. The protein levels were quantified with a BCA protein assay kit (Beyotime Biotechnology, Shanghai, China). Then, the samples were electrophoresed in SD-PAGE to separate protein bands. Proteins were transferred from the gel onto PVDF membranes and blocked with 5% nonfat dry milk for 2 h. The membrane was incubated with the first antibody (1 : 1000, Abcam, Cambridge, UK) for overnight at 4°C and then a second antibody (Thermo Fisher Scientific, Shanghai, China) for 2 h.

Later, bands were visualized by exposure to ECL method, and the overall gray value of protein bands was quantified actin as an internal marker, namely, target protein gray value/internal reference overall gray value.

2.9. Quantitative Real-Time PCR. We followed the methods of Wang et al. [24, 25]. Total RNA was extracted with TRIzol and assessed by spectrophotometer. Then, reverse transcription of RNA from each group was performed using Prime Script RT reagent Kit (Beyotime Biotechnology, Shanghai, China). Primer was designed and synthesized by Shanghai Biotechnology Service Company in accordance with Gene sequence in GenBank Gene sequence design, together with Oligo v6.6 (sequences as Table 1). qPCR was performed using Premix Ex Taq SYBR-Green PCR (Takara) according to the manufacturer's instructions on an ABI PRISM 7300 (Applied Biosystems, Foster City, CA, USA). The mRNA level of individual genes was normalized to GAPDH and calculated by $2^{-\Delta\Delta CT}$ data analysis method.

2.10. Statistical Analysis. Statistical analysis was performed using GraphPad Prism 6.0 Software (San Diego, CA, USA). Data are presented as mean ± standard deviation (SD). Group comparisons were assessed with one-way ANOVA or Student's t-test with Bonferroni's post hoc test for comparison of multiple columns. A value of $P < 0.05$ (two-tailed) was considered statistically significant. Higher significance levels were established at $P < 0.01$.

3. Results

3.1. Agnuside Relieves the State of Hypoxia in KOA Rats. The chemical structure of AGN is shown as Figure 1(a). Similar to our previous study, the synovial tissues of MIA-induced KOA model rats showed aggravated hypoxia compared with the normal group observed by pimonidazole staining. AGN (6.25 mg/kg) could be able to relieve this situation (Figure 1(b)). Subsequently, immunohistochemistry was performed to evaluate the protein expression of HIF-1α in

TABLE 1: Nucleotide sequences of primers used for RT-PCR amplification.

Target gene	Forward primer	Reverse primer
HIF-1α	CCGCAACTGCCACCACTGATG	TGAGGCTGTCCGACTGTGAGTAC
Caspase-1	ATGGCCGACAAGGTCCTGAGG	GTGACATGATCGCACAGGTCTCG
NLRP3	GAGCTGGACCTCAGTGACAATGC	ACCAATGCGAGATCCTGACAACAC
ASC	AGAGTCTGGAGCTGTGGCTACTG	ATGAGTGCTTGCCTGTGTTGGTC
TGF-β	GCAACAATTCCTGGCGTTACCTTG	TGTATTCCGTCTCCTTGGTTCAGC
VEGF	AGCGTTCACTGTGAGCCTTGTTC	CCGCCTTGGCTTGTCACATCTG
TIMP1	GCGTTCTGCAACTCGGACCTG	GTGTAGGCGAACCGGATATCTGTG
GAPDH	GGCCTTCCGTGTTCCTACC	ACTCGACACCTGCCCTCA

synovial tissue (Figures 1(c) and 1(d)). The percentage of HIF-1α-positive areas in the KOA group showed a significant upregulation compared with the normal group ($P < 0.05$), while the KOA+AGN group showed a significant downregulation compared with the KOA group ($P < 0.05$). The mRNA levels of HIF-1α measured by PCR in each group were consistent with the immunohistochemistry assay (Figure 1(e)).

3.2. Agnuside May Inhibit NLRP3 Inflammasome and Alleviate Synovitis in KOA Rats. To observe the effect of AGN on NLRP3 inflammasome in KOA, PCR and WB were performed to quantitatively study the expression of pro-caspase-1, caspase-1 p10, ASC, and NLRP3 protein (Figures 2(a)–2(c)). Both the mRNA and protein levels of these substances in the KOA group were significantly higher than the normal group ($P < 0.05$), and the KOA+AGN group resulted in a reduced expression compared with the KOA group ($P < 0.05$). Subsequently, we analyzed the serum content of IL-1β and IL-18 in each group with ELISA (Figure 2(d)). As the downstream of NLRP3 inflammasome activation, these proinflammatory factors resulted in an upregulation in the KOA group compared with the normal group ($P < 0.05$) while the KOA+AGN group showed a significant downregulation compared with the KOA group ($P < 0.05$). Besides, we evaluated synovial inflammation overall in all groups of rats. Under the observation of HE sections, the KOA+AGN group showed orderly arranged synovial lining cells, loose connective tissue, and less inflammatory cell infiltration compared with the KOA group (Figure 2(e)). Same results were obtained from the synovitis score according to Kenn's criteria in scoring HE sections (Figure 2(f)).

3.3. Agnuside Alleviates Synovial Fibrosis in KOA Rats. To evaluate the effect of AGN on synovial fibrosis in KOA, anatomical characteristics and pathological sections of synovial tissue were observed. The KOA group showed markedly increased collagen deposition, while this change was relatively lessened in the KOA+AGN group observed under anatomy (Figure 3(a)). The same results can be observed by Sirius Red staining (Figure 3(b)). Subsequently, we performed a semiquantitative analysis by immunohistochemical staining of type I collagen (Figures 3(c) and 3(d)). In the KOA group, the percentage of collagen I-positive areas was significantly higher in comparison with the normal group

($P < 0.05$). But in the KOA+AGN group, collagen I deposition was significantly alleviated compared with the KOA group ($P < 0.05$). More specifically, we measured both mRNA and protein expressions of fibrotic markers TGF-β, TIMP1, and VEGF in synovial tissues (Figures 3(e)–3(g)). We found that there was a significant decrease level of profibrotic substances in the KOA+AGN group.

3.4. Agnuside Inhibits HIF-1α Accumulation and NLRP3 Inflammasome Activation in LPS-Treated FLSs. The LPS-induced model of FLSs was established mimicking the inflammatory environment of KOA and activating NLRP3 inflammasome. We first observed the effect of AGN on the caspase-1 activity in KOA FLSs (Figure 4(a)). LPS stimulation significantly increased the activity of caspase-1 in normal FLSs, and AGN (3 μm) significantly reduced the increased caspase-1 activity of LPS challenge ($P < 0.05$). Furthermore, we investigated the effects of AGN on HIF-1α and NLRP3 inflammasome components in vitro (Figures 4(b)–4(d)). In the LPS group, both mRNA and protein levels of HIF-1α were upregulated compared with the normal ($P < 0.05$), AGN significantly prevented this upregulation ($P < 0.05$). LPS also promoted the mRNA expression of caspase-1, ASC, and NLRP3, and this trend was reversed by AGN. Same changes occurred in protein expression, not only the precursors of caspase-1 but also the cleavage caspase-1 p10. In addition, we studied the effect of AGN on the downstream product of NLRP3 inflammasome activation. The content of IL-1β and IL-18 (Figure 4(e)) in the supernatant of the LPS+AGN group was significantly lower than that in the LPS group ($P < 0.05$).

3.5. Agnuside Downregulates Fibrosis Marker Expression in LPS-Treated FLSs. After AGN-treated for 24 hours, both mRNA and protein expressions of TGF-β, TIMP1, and VEGF in FLSs were assessed (Figures 5(a)–5(c)). These fibrosis markers showed a significant upregulation in the LPS group compared with the normal group ($P < 0.05$), and the LPS+AGN group resulted in a downregulation compared with the LPS group ($P < 0.05$).

4. Discussion

The current study indicates that AGN may alleviate synovitis and fibrosis in KOA through the inhibition of HIF-1α
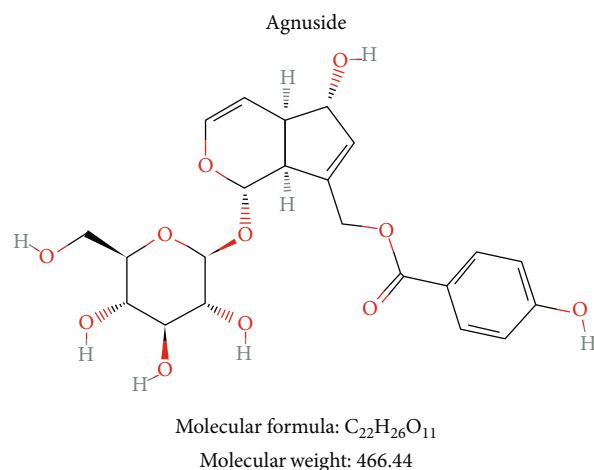
(a)
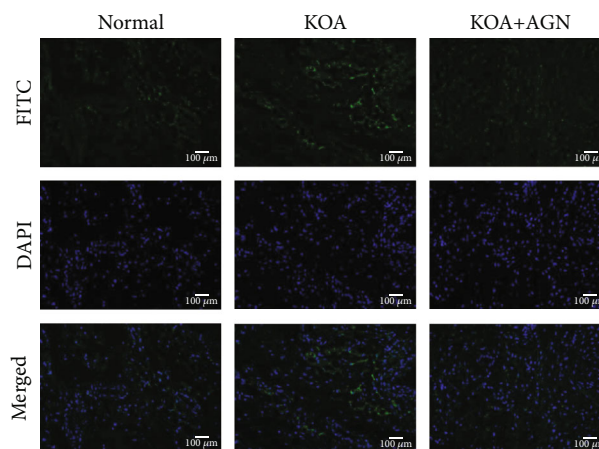
(b)
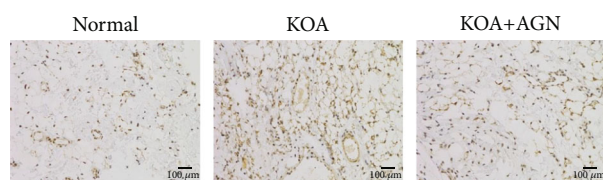
(c)
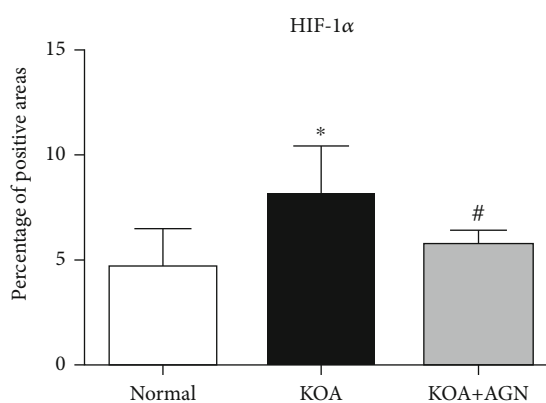
(d)
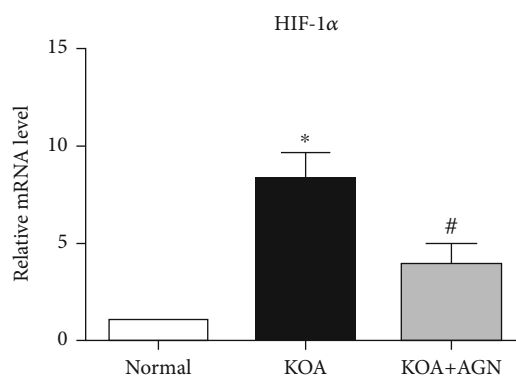
(e)

Figure 1: Agnuside relieves the state of hypoxia in KOA rats. (a) The chemical structure of AGN. (b) Representative synovial tissues stained with pimonidazole, 200x, scale bar = 100 μm. (c) Representative HIF-1α immunohistochemical sections of synovial tissues in each group, 200x, scale bar = 100 μm. (d) The percentage of HIF-1α-positive areas in each group. Data were analyzed by ImageJ. $^*P < 0.05$, compared with the normal group. $^\#P < 0.05$, compared with the KOA group. (e) mRNA level of HIF-1α between groups. $^*P < 0.05$ compared with the normal group. $^\#P < 0.05$, compared with the KOA group.

accumulation and NLRP3 inflammasome activation. According to our literature search, the number of studies on AGN is very small. Fortunately, these few studies have provided us with the effective dose of AGN in vivo and in vitro, the time of intervention, distribution in vivo, and so on, which provide great convenience for our work [19, 20]. Therefore, we chose an oral dose at 6.25 mg/kg and a cel-

lular dose of 3 μM to continue our experiment. We select MIA intra-articular injection to construct the KOA model. MIA induces cartilage degeneration and subchondral bone sclerosis, which mimics the pathological changes observed in human OA [26]. More importantly, synovitis and fibrosis in the MIA method develop rapidly compared with surgical modeling such as anterior cruciate ligament or meniscus

(a)

(b)

(c)

(d)

(e)

(f)
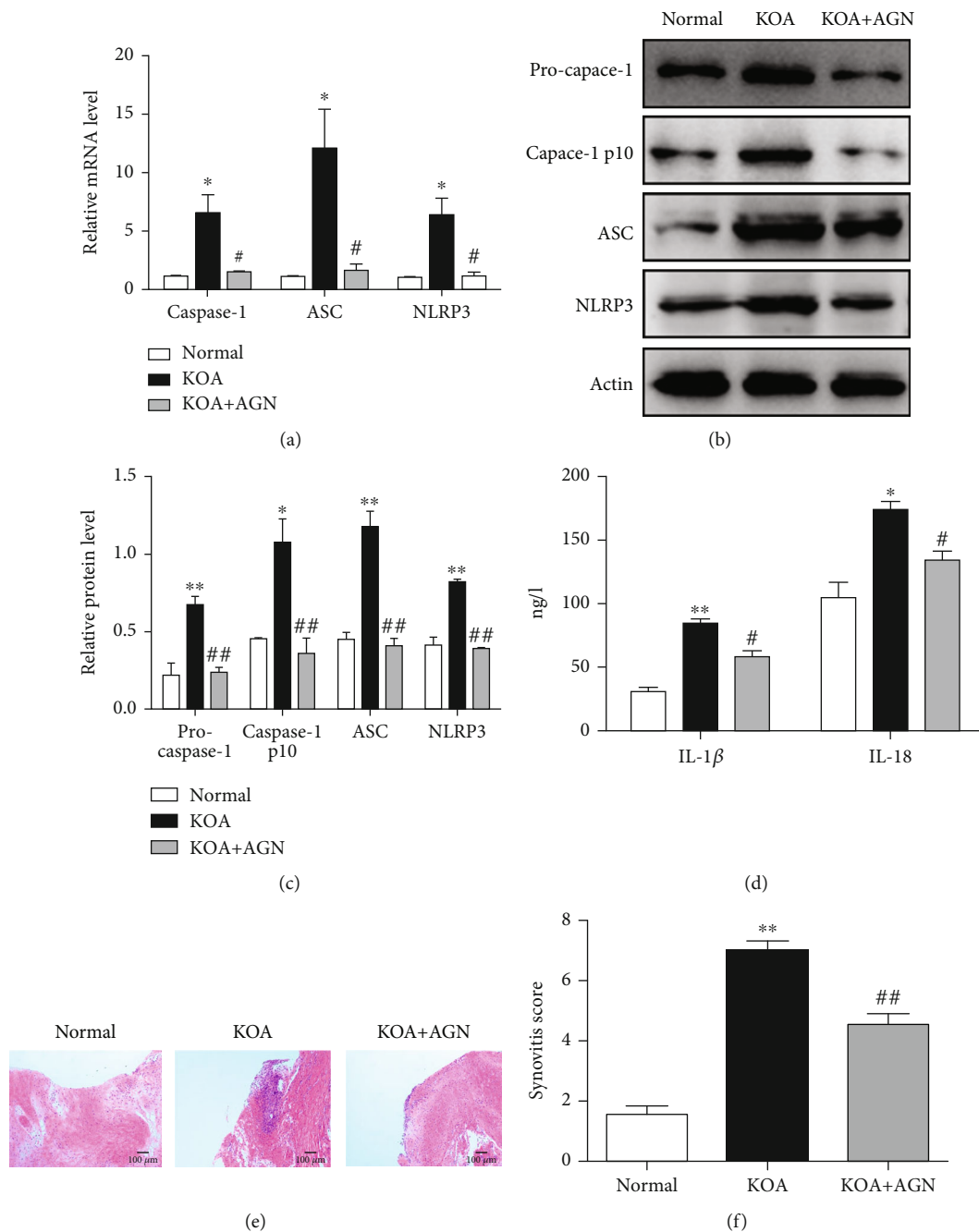
FIGURE 2: Agnuside may inhibit NLRP3 inflammasome and alleviate synovitis in KOA Rats. (a) mRNA levels of caspase-1, ASC, and NLRP3 in each group. $^*P < 0.05$, in comparison with the normal group. $^#P < 0.05$, in comparison with the KOA group. (b) Typical protein bands for each group. (c) Protein level comparison of pro-caspase-1, caspase-1, p10, ASC, and NLRP3 between groups. $^*P < 0.05$, $^{**}P < 0.01$, compared with the normal group. $^{##}P < 0.01$, compared with the KOA group. (d) Serum levels of IL-1β and IL-18 between groups. $^*P < 0.05$, $^{**}P < 0.01$, compared with the normal group. $^#P < 0.05$, compared with the KOA group. (e) Representative synovial tissues of each group stained with stained with HE staining, 200x, scale bar = 100 μm. (f) Synovitis score according to Kenn's criteria. $^{**}P < 0.01$, compared with the normal group. $^{##}P < 0.01$, compared with the KOA group.

resection; it could be more suitable to research the effect of AGN intervention. For the same reason, we selected LPS at the dose of 10 μg/ml to operate in vitro experiments.

To the best of our knowledge, this may be the first study to reveal the target of AGN efficacy. Previous studies have focused more on the extraction and purification of AGN from a chaste trees (Vitex agnus cactus L., Family Verbena-

ceae), or a preliminary observation on the anti-inflammatory and antioxidant capacity of AGN. In this study, we revealed that HIF-1α and NLRP3 inflammasomes are effective intervention targets for AGN. We also conducted a series of quantitative studies to demonstrate that AGN prevents HIF-1α accumulation and NLRP3 inflammasome activation, thereby alleviating KOA synovitis and
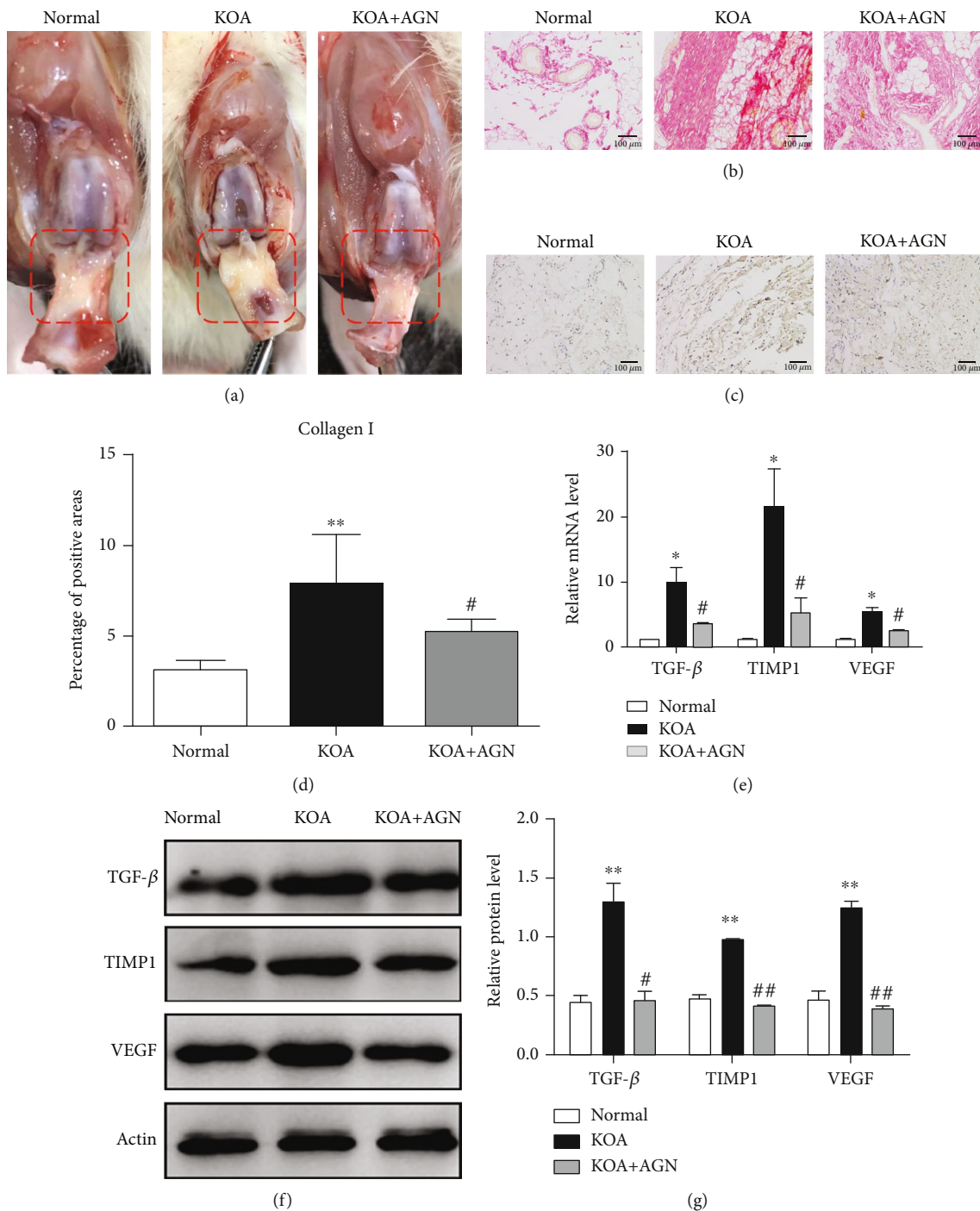
FIGURE 3: Agnuside alleviates synovial fibrosis in KOA rats. (a) Anatomical changes of synovial tissues (red box area) in each group. (b) Collagen deposition was revealed through Sirius Red staining, 200x, scale bar = 100 μm. (c) Representative type I collagen immunohistochemical sections of synovial tissues in each group, 200x, scale bar = 100 μm. (d) Semiquantification of immunohistochemical sections was evaluated by calculating the percentage of collagen I-positive areas. $^{**}P < 0.01$, in comparison with the normal group. $^{#}P < 0.05$, in comparison with the KOA group. Data were analyzed by ImageJ. (e) Comparison of TGF-β, TIMP1, and VEGF mRNA levels between groups. $^{*}P < 0.05$, compared with the normal group. $^{#}P < 0.05$, compared with the KOA group. (f) Typical protein bands for each group. (g) Comparison of TGF-β, TIMP1, and VEGF protein expressions between groups. $^{**}P < 0.01$, compared with the normal group. $^{#}P < 0.05$, $^{##}P < 0.01$, compared with the KOA group.

fibrosis. Since the symptoms of KOA are directly related to the severity of synovitis and fibrosis, the findings of this paper may suggest a potential value in KOA treatment.

As a motor joint, it is widely accepted that the local tissue of the KOA joint is deficient in oxygen [27]. When oxygen demand exceeds supply, a cascade of intracellular events is

(a)   (b)   (c)

(d)   (e)
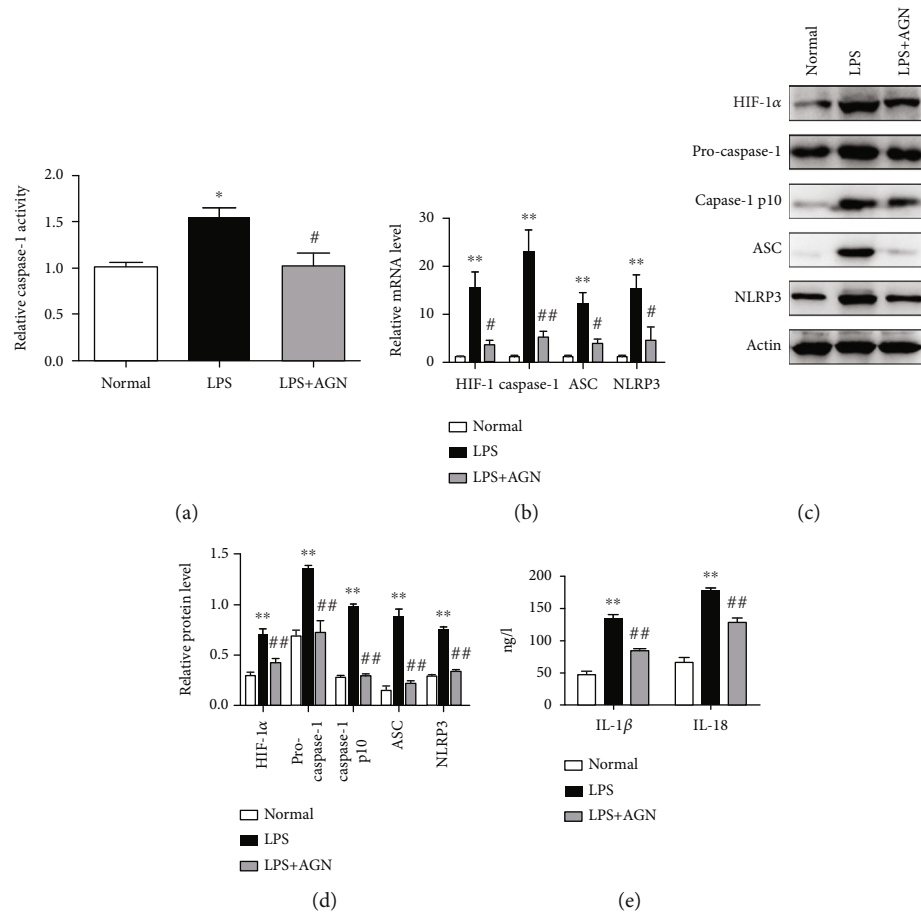
Figure 4: Agnuside inhibits HIF-1α accumulation and NLRP3 inflammasome activation in LPS-treated FLSs. (a) Relative caspase-1 activity for each group. $^*P < 0.05$, in comparison with the normal group. $^{\#}P < 0.05$, in comparison with the LPS group. (b) mRNA level of HIF-1α, caspase-1, ASC, and NLRP3 in each group. $^*P < 0.05$, $^{**}P < 0.01$, in comparison with the normal group. $^{\#}P < 0.05$, $^{\#\#}P < 0.01$, in comparison with the KOA group. (c) Typical protein bands for each group. (d) Protein level comparison of HIF-1α, pro-caspase-1, caspase-1 p10, ASC, and NLRP3 between groups. $^{**}P < 0.01$, compared with the normal group. $^{\#\#}P < 0.01$, compared with the KOA group. (e) FLS supernatant contents of IL-1β and IL-18 between groups. $^{**}P < 0.01$, compared with the normal group. $^{\#\#}P < 0.01$, compared with the KOA group.

activated, increasing the expression of HIF-1α. Qing et al. proved that the expression of HIF-1α in the synovial fluid and articular cartilage is associated with the disease severity in KOA [28]. HIF-1α promotes the development of inflammation; besides, as a transcription factor, HIF-1α directly regulates the expression of genes encoding proteins involved in fibrosis, such as TGF-β and VEGF [29]. Thus, hypoxia may be common upstream of synovitis and fibrosis in KOA. A variety of plant extracts have antioxidant properties, in our study; AGN, a compound isolated from the extract of Vitex negundo L., significantly improved the oxygen-containing state of synovial tissue in KOA rats. Our findings are based on the direct observation of anoxic probes and the quantitative detection of HIF-1α; in vitro experiments with FLSs yielded the same conclusions. These evidences suggest that AGN can reduce the accumulation of HIF-1α.

NLRP3 inflammasome activation may be one of the consequences of HIF-1α accumulation [30]. How to relieve local inflammation by inhibiting NLRP3 has also become a focus of anti-inflammatory therapy due to the critical role of

NLRP3 in mediating inflammatory cascade amplification. A variety of herbal or herbal extracts have been confirmed benign intervention on NLRP3 inflammasome. Wang et al. studied the effect of isochlorogenic acid A intervention on NLRP3 inflammasome in an acute lung injury model and proved the expressions of NF-κB/NLRP3 signaling pathway were inhibited by isochlorogenic acid A [31]. Huang et al. demonstrated that salvianolic acid B suppressed oxidative stress and neuroinflammation via regulating NLRP3 inflammasome activation [32]. Besides, Coptidis Rhizoma and others all have anti-inflammatory effects by targeting NLRP3 inflammasome [33–35]. In this study, we confirmed that AGN decreased caspase-1 activity and the protein level of cleaved caspase-1 (caspase-1 p10). Moreover, AGN was able to reduce both gene and protein expressions of caspase-1, ASC, and NLRP3 proteins, which assemble NLRP3 inflammasome during activation. Meanwhile, proinflammatory factors IL-1β and IL-18, downstream of NLRP3 inflammasome activation, were also downregulated after AGN intervention. Our results indicate that AGN may attenuate synovitis by inhibiting NLRP3 activation in KOA.
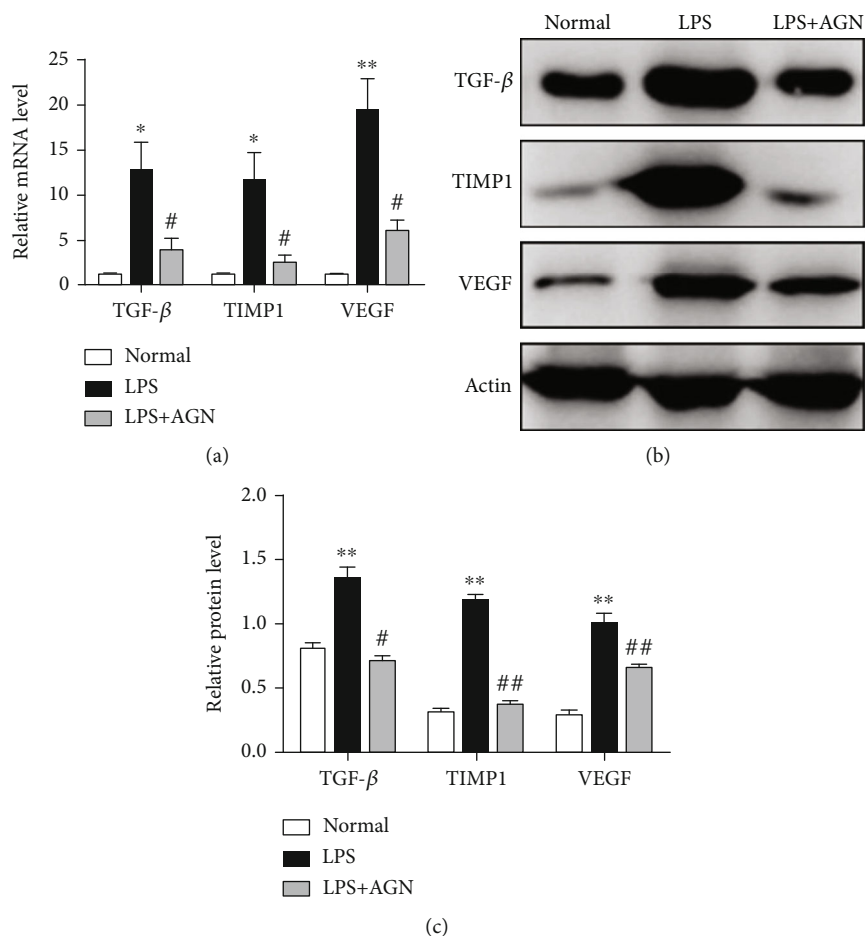
(a)

(b)

(c)

FIGURE 5: Agnuside downregulates fibrosis marker expression in LPS-treated FLSs. (a) Relative mRNA levels of TGF-β, TIMP1, and VEGF in FLSs in each group. $^*P < 0.05$, $^{**}P < 0.01$, in comparison with the normal group. $^\#P < 0.05$, in comparison with the KOA group. (b) Typical protein bands for each group. (c) Comparison of TGF-β, TIMP1, and VEGF protein expressions between groups. $^{**}P < 0.01$, compared with the normal group. $^\#P < 0.05$, $^{\#\#}P < 0.01$, compared with the KOA group.

Increasing evidence has shown that NLRP3 inflammasome activation in different tissues such as the liver, renal, and airway participates in chronic aseptic inflammation and can be related to tissue fibrosis. The response to TGF-β is a key event in the onset of synovial fibrosis in KOA, in addition to TIMP1 and VEGF, which are important indicators for evaluating synovial fibrosis [36]. Antifibrosis therapy can play a positive role in the prevention and treatment of joint stiffness. Accordingly, we first examined the effect of AGN on fibrosis under anatomical observations; synovial tissue in rats with AGN intervention showed less collagen deposition. The same results can be observed by Sirius Red staining or immunohistochemical staining of type I collagen. Subsequently, we measured both the mRNA and protein expressions of TGF-β, TIMP1, and VEGF to evaluate fibrosis in vivo and in vitro. AGN-treated group showed a downregulation of all these profibrotic substances compared to the KOA group. Our results support the antifibrotic effect of AGN, which is likely to be achieved by inhibiting NLRP3 inflammasome activation.

The current study still has a few limitations. First, the effects of different doses or concentrations of AGN on KOA synovitis and fibrosis were not examined. This is because on the one hand, other studies have made a detailed observation; on the other hand, we were not very sure whether AGN can act on HIF-1α or NLRP3 inflammasome. Secondly, we did not set up a positive control group, and the difference in efficacy between monomers was not the focus of our study. Besides, the sample size of experimental animals would be bigger if possible.

5. Conclusion

In summary, this study demonstrates that AGN alleviates synovitis and fibrosis in experimental KOA through the inhibition of HIF-1α accumulation and NLRP3 inflammasome activation. Additionally, not only does it reveal some novel targets for anti-inflammatory and antioxidant effects of AGN but also announces its potential value in treating KOA in humans.

Abbreviations

KOA: Knee osteoarthritis

HIF-1α: Hypoxia-inducible transcription factor-1α
NLRP: Nucleotide-binding and oligomerization domain-
           like receptor family pyrin domain-containing
ASC: Apoptosis-associated speck-like protein with a
           caspase-recruitment domain
AGN: Agnuside
TGF-β: Transforming growth factor-β
TIMP1:   Tissue inhibitor of metalloproteinases 1
VEGF: Vascular endothelial growth factor
FLSs: Fibroblast-like synoviocytes
LPS: Lipopolysaccharide
ATP: Adenosine triphosphate.

Data Availability

The data used to support the findings of this study are available from the corresponding author upon request.

Conflicts of Interest

All authors declare that there are no actual or potential conflicts of interest, including any financial, personal, or other relationships with other people or organizations that could inappropriately influence, or be perceived to influence our work.

Acknowledgments

References

[1] R. J. Miller, A. M. Malfait, and R. E. Miller, "The innate immune response as a mediator of osteoarthritis pain," *Osteoarthritis and Cartilage*, vol. 28, no. 5, pp. 562–571, 2020.

[2] S. Glyn-Jones, A. J. Palmer, R. Agricola et al., "Osteoarthritis," *Lancet.*, vol. 386, no. 9991, pp. 376–387, 2015.

[3] J. R. Anderson, S. Chokesuwattanaskul, M. M. Phelan et al., "1H NMR metabolomics identifies underlying inflammatory pathology in osteoarthritis and rheumatoid arthritis synovial joints," *Journal of Proteome Research*, vol. 17, no. 11, pp. 3780–3790, 2018.

[4] F. J. Zhang, W. Luo, and G. H. Lei, "Role of HIF-1α and HIF-2α in osteoarthritis," *Joint, Bone, Spine*, vol. 82, no. 3, pp. 144–147, 2015.

[5] L. Zhang, L. Zhang, Z. Huang et al., "Increased HIF-1α in knee osteoarthritis aggravate synovial fibrosis via fibroblast-like synoviocyte pyroptosis," *Oxidative Medicine and Cellular Longevity*, vol. 2019, Article ID 6326517, 11 pages, 2019.

[6] L. Spel and F. Martinon, "Inflammasomes contributing to inflammation in arthritis," *Immunological Reviews*, vol. 294, no. 1, pp. 48–62, 2020.

[7] F. Liang, F. Zhang, L. Zhang, and W. Wei, "The advances in pyroptosis initiated by inflammasome in inflammatory and immune diseases," *Inflammation Research*, vol. 69, no. 2, pp. 159–166, 2020.

[8] J. Wu, S. Lin, B. Wan, B. Velani, and Y. Zhu, "Pyroptosis in liver disease: new insights into disease mechanisms," *Aging and Disease*, vol. 10, no. 5, pp. 1094–1108, 2019.

[9] E. Theofani, M. Semitekolou, I. Morianos, K. Samitas, and G. Xanthou, "Targeting NLRP3 inflammasome activation in severe asthma," *Journal of Clinical Medicine*, vol. 8, no. 10, p. 1615, 2019.

[10] H. Zhang and Z. Wang, "Effect and regulation of the NLRP3 inflammasome during renal fibrosis," *Frontiers in Cell and Development Biology*, vol. 7, 2020.

[11] D. F. Remst, E. N. Blaney Davidson, and P. M. van der Kraan, "Unravelling osteoarthritis-related synovial fibrosis: a step closer to solving joint stiffness," *Rheumatology*, vol. 54, no. 11, pp. 1954–1963, 2015.

[12] P. M. van der Kraan, "The changing role of TGFβ in healthy, ageing and osteoarthritic joints," *Nature Reviews Rheumatology*, vol. 13, no. 3, pp. 155–163, 2017.

[13] C. Song, X. Xu, Y. Wu, B. Ji, X. Zhou, and L. Qin, "Study of the mechanism underlying hsa-miR338-3p downregulation to promote fibrosis of the synovial tissue in osteoarthritis patients," *Molecular Biology Reports*, vol. 46, no. 1, pp. 627–637, 2019.

[14] Y. Chen, F. Qiu, X. Zhu, H. Mo, Z. Wu, and C. Xiao, "Pannus does not occur only in rheumatoid arthritis: a pathological observation of pannus of knee osteoarthritis," *Journal of Southern Medical University*, vol. 39, no. 6, pp. 747–750, 2019.

[15] E. Sharma, N. Tyagi, V. Gupta, A. Narwal, H. Vij, and D. Lakhnotra, "Role of angiogenesis in oral submucous fibrosis using vascular endothelial growth factor and CD34: an immunohistochemical study," *Indian Journal of Dental Research*, vol. 30, no. 5, pp. 755–762, 2019.

[16] P. Wu, Z. Huang, J. Shan et al., "Interventional effects of the direct application of "Sanse powder" on knee osteoarthritis in rats as determined from lipidomics via UPLC-Q-Exactive Orbitrap MS," *Chinese Medicine*, vol. 15, no. 1, 2020.

[17] S. Shah, T. Dhanani, and S. Kumar, "Validated HPLC method for identification and quantification of _p_ -hydroxy benzoic acid and agnuside in _Vitex negundo_ and _Vitex trifolia_," *Journal of Pharmaceutical Analysis*, vol. 3, no. 6, pp. 500–508, 2013.

[18] N. Tiwari, S. Luqman, N. Masood, and M. M. Gupta, "Validated high performance thin layer chromatographic method for simultaneous quantification of major iridoids in _Vitex trifolia_ and their antioxidant studies," *Journal of Pharmaceutical and Biomedical Analysis*, vol. 61, pp. 207–214, 2012.

[19] R. Ramakrishna, M. Bhateria, R. Singh, S. K. Puttrevu, and R. S. Bhatta, "Plasma pharmacokinetics, bioavailability and tissue distribution of agnuside following peroral and intravenous administration in mice using liquid chromatography tandem mass spectrometry," *Journal of Pharmaceutical and Biomedical Analysis*, vol. 125, pp. 154–164, 2016.

[20] A. Pandey, S. Bani, N. K. Satti, B. D. Gupta, and K. A. Suri, "Anti-arthritic activity of agnuside mediated through the down-regulation of inflammatory mediators and cytokines," *Inflammation Research*, vol. 61, no. 4, pp. 293–304, 2012.

[21] V. Krenn, L. Morawietz, G. R. Burmester et al., "Synovitis score: discrimination between chronic low-grade and high-grade synovitis," *Histopathology*, vol. 49, no. 4, pp. 358–364, 2006.

[22] X. Li, W. Mei, Z. Huang et al., "Casticin suppresses monoiodoacetic acid-induced knee osteoarthritis through inhibiting

HIF-1α/NLRP3 inflammasome signaling," *International Immunopharmacology*, vol. 86, article 106745, 2020.

[23] L. R. Zhao, R. L. Xing, P. M. Wang et al., "NLRP1 and NLRP3 inflammasomes mediate LPS/ATP-induced pyroptosis in knee osteoarthritis," *Molecular Medicine Reports*, vol. 17, no. 4, pp. 5463–5469, 2018.

[24] T. Liao, L. Ding, P. Wu et al., "Chrysin attenuates the NLRP3 inflammasome cascade to reduce synovitis and pain in KOA rats," *Drug Design, Development and Therapy*, vol. 14, pp. 3015–3027, 2020.

[25] L. Zhang, R. Xing, Z. Huang et al., "Inhibition of synovial macrophage pyroptosis alleviates synovitis and fibrosis in knee osteoarthritis," *Mediators of Inflammation*, vol. 2019, Article ID 2165918, 11 pages, 2019.

[26] J. E. Kim, D. H. Song, S. H. Kim, Y. Jung, and S. J. Kim, "Development and characterization of various osteoarthritis models for tissue engineering," *PLoS One*, vol. 13, no. 3, article e0194288, 2018.

[27] Z. Liu, M. Au, X. Wang et al., "Photoacoustic imaging of synovial tissue hypoxia in experimental post- traumatic osteoarthritis," *Progress in Biophysics and Molecular Biology*, vol. 148, pp. 12–20, 2019.

[28] L. Qing, P. Lei, H. Liu et al., "Expression of hypoxia-inducible factor-1α in synovial fluid and articular cartilage is associated with disease severity in knee osteoarthritis," *Experimental and Therapeutic Medicine*, vol. 13, no. 1, pp. 63–68, 2017.

[29] J. Fernández-Torres, G. A. Martínez-Nava, M. C. Gutiérrez-Ruíz, L. E. Gómez-Quiroz, and M. Gutiérrez, "Papel da via de sinalizaçao do HIF-1α na osteoartrite: revisao sistematica," *Revista Brasileira de Reumatologia (English Edition)*, vol. 57, no. 2, pp. 162–173, 2017.

[30] Mian Wu, M. Zhang, Y. Ma et al., "Chaetocin attenuates gout in mice through inhibiting HIF-1α and NLRP3 inflammasome-dependent IL-1β secretion in macrophages," *Archives of Biochemistry and Biophysics*, vol. 670, pp. 94–103, 2019.

[31] Q. Wang and L. Xiao, "Isochlorogenic acid A attenuates acute lung injury induced by LPS via Nf-κB/NLRP3 signaling pathway," *American Journal of Translational Research*, vol. 11, no. 11, pp. 7018–7026, 2019.

[32] Q. Huang, X. Ye, L. Wang, and J. Pan, "Salvianolic acid B abolished chronic mild stress-induced depression through suppressing oxidative stress and neuro-inflammation via regulating NLRP3 inflammasome activation," *Journal of Food Biochemistry*, vol. 43, no. 3, article e12742, 2019.

[33] Y. Ren, D. Wang, F. Lu et al., "Coptidis Rhizoma_ inhibits NLRP3 inflammasome activation and alleviates renal damage in early obesity-related glomerulopathy," *Phytomedicine*, vol. 49, pp. 52–65, 2018.

[34] H. He, H. Jiang, Y. Chen et al., "Oridonin is a covalent NLRP3 inhibitor with strong anti-inflammasome activity," *Nature Communications*, vol. 9, no. 1, 2018.

[35] Y. Liu, Y. Y. Jing, C. Y. Zeng et al., "Scutellarin suppresses NLRP3 inflammasome activation in macrophages and protects mice against bacterial sepsis," *Frontiers in Pharmacology*, vol. 8, 2018.

[36] M. Lodyga and B. Hinz, "TGF-β1 - a truly transforming growth factor in fibrosis and immunity," *Seminars in Cell & Developmental Biology*, vol. 101, pp. 123–139, 2020.

Research Article

Interleukin-22 Plays a Protective Role by Regulating the JAK2-STAT3 Pathway to Improve Inflammation, Oxidative Stress, and Neuronal Apoptosis following Cerebral Ischemia-Reperfusion Injury

Yongfei Dong [iD],[1] Chengyun Hu,[2] Chunxia Huang,[3] Jie Gao,[4] Wanxiang Niu,[5] Di Wang,[3] Yang Wang,[5] and Chaoshi Niu [iD][6]

[1]*Department of Neurosurgery, Anhui Provincial Hospital, Cheeloo College of Medicine, Shangdong University, Jinan, Shangdong, 250021, China*
[2]*Department of Anesthesiology, The First Affiliated Hospital of USTC, Division of Life Sciences and Medicine, University of Science and Technology of China, Hefei, Anhui 230001, China*
[3]*Department of Anesthesiology, The Second Affiliated Hospital of Anhui Medical University, Hefei, Anhui 230601, China*
[4]*Department of Anesthesiology, The First Affiliated Hospital of Anhui Medical University, Hefei, Anhui 230022, China*
[5]*Department of Neurosurgery, The First Affiliated Hospital of USTC, Division of Life Sciences and Medicine, University of Science and Technology of China, Hefei, Anhui 230001, China*
[6]*Department of Neurosurgery, Anhui Provincial Hospital, Hefei, Anhui 230001, China*

Correspondence should be addressed to Chaoshi Niu; niuchaoshi@126.com

Academic Editor: Antonela Romina Terrizzi

The interleukins (ILs) are a pluripotent cytokine family that have been reported to regulate ischemic stroke and cerebral ischemia/reperfusion (I/R) injury. IL-22 is a member of the IL-10 superfamily and plays important roles in tissue injury and repair. However, the effects of IL-22 on ischemic stroke and cerebral I/R injury remain unclear. In the current study, we provided direct evidence that IL-22 treatment decreased infarct size, neurological deficits, and brain water content in mice subjected to cerebral I/R injury. IL-22 treatment remarkably reduced the expression of inflammatory cytokines, including IL-1β, monocyte chemotactic protein- (MCP-) 1, and tumor necrosis factor- (TNF-) α, both in serum and the ischemic cerebral cortex. In addition, IL-22 treatment also decreased oxidative stress and neuronal apoptosis in mice after cerebral I/R injury. Moreover, IL-22 treatment significantly increased Janus tyrosine kinase (JAK) 2 and signal transducer and activator of transcription (STAT) 3 phosphorylation levels in mice and PC12 cells, and STAT3 knockdown abolished the IL-22-mediated neuroprotective function. These findings suggest that IL-22 might be exploited as a potential therapeutic agent for ischemic stroke and cerebral I/R injury.

1. Introduction

A report from the Global Burden of Disease (GBD) 2016 Stroke Collaborators showed that although the prevalence and mortality of stroke have decreased in the past 20 years, stroke remains the second leading cause of death and long-term disability worldwide [1, 2]. Among them, ischemic stroke is the most common type and occurs when cerebral arteries are occluded [3, 4]. Currently, restoring blood perfusion is an approved therapy for cerebral ischemic injury, including intravenous thrombolytic and endovascular therapy [5–8]. However, the degree of brain injury may be further aggravated following the reperfusion process, which is called cerebral ischemia/reperfusion (I/R) injury [9, 10]. Increasing

evidence has shown that cerebral I/R can cause secondary brain injury, including cerebral hemorrhage, cerebral edema, and even death [11, 12]. Thus, it is necessary to clarify the pathological mechanism underlying cerebral I/R injury and explore novel therapeutic agents for ischemic stroke and cerebral I/R injury.

The interleukins (ILs) are a pluripotent cytokine family that have been reported to regulate ischemic stroke and cerebral I/R injury [13, 14]. In clinical experiments, higher IL-33 levels in acute ischemic stroke patients were positively correlated with better prognosis and could be used to predict outcomes and recurrences in acute ischemic stroke patients [15]. In addition, an IL-1 receptor antagonist (IL-1Ra) significantly decreased plasma concentrations of IL-6 and C-reactive protein in patients with ischemic stroke, indicating that IL-1Ra can improve clinical outcomes by reducing inflammation [16]. IL-35 pretreatment significantly reduced brain infarction and neurological deficits after cerebral I/R injury [17]. In addition, inhibition of IL-32 significantly reduced the infarct volume and neurological deficits following cerebral I/R injury by suppressing proinflammatory cytokine secretion [18].

IL-22 is a member of the IL-10 superfamily and plays important roles in tissue injury and repair [19, 20]. IL-22 has been reported to participate in various biological processes, including the inflammatory response, oxidative stress, endoplasmic reticulum stress, autophagy, apoptosis, and cell death [21–24]. Takahashi et al. reported that IL-22 treatment ameliorated I/R-induced myocardial injury and apoptosis by activating the signal transducer and activator of transcription (STAT) 3 signaling pathway [25]. Xu et al. also reported that IL-22 treatment or IL-22 overexpression prevented renal injury and inflammation after renal I/R in mice [26]. However, it remains unclear whether IL-22 is involved in ischemic stroke and cerebral I/R injury. Thus, the aim of this study was to determine the roles of IL-22 in cerebral I/R injury and to explore the underlying mechanism.

2. Materials and Methods

2.1. Animals and Animal Model. Male C57BL/6J mice were purchased from Beijing HFK Biotechnology Co., Ltd. (Beijing, China). All mice were maintained in standard housing conditions under a 12 h light-dark cycle and were allowed free access to standard rodent food and water. Animal care and procedures were conducted in accordance with the NIH *Guide for the Care and Use of Laboratory Animals* and approved by the Animal Ethics Committee of Anhui Medical University.

A middle cerebral artery occlusion (MCAO) model was generated according to previous research [27]. After 45 min of ischemia, the suture was removed to initiate reperfusion. The sham-operated mice underwent the same procedures but did not receive sutures. Thirty minutes before reperfusion, the mice were injected intraperitoneally with recombinant mouse IL-22 protein (rIL-22). The doses and times were selected according to our pilot experiments and previous research. The 90 mice were randomly allocated into the

following three groups ($n = 30$/group): sham group, MCAO group, and rIL-22 group.

2.2. Neurological Impairment Scores. After 24 h of reperfusion, neurological impairment was evaluated as previously described [28]. The neurological scoring system ranged from 0 (no neurological deficits) to 4 (inability to walk spontaneously).

2.3. Measurement of Infarct Area. After neurological evaluation, the brains were rapidly removed and subsequently cut into coronal sections and then incubated with 2,3,5-triphenyltetrazolium chloride (TTC) at 37°C for 20 min. The sections were fixed in 4% paraformaldehyde and photographed using an HD camera. The infarct area was analyzed using ImageJ, and the infarct volume was calculated as previously described [29].

2.4. Brain Water Content. After 24 h of reperfusion, the mice were sacrificed and the brain tissues were rapidly removed and then immediately weighed to obtain the wet weight. Subsequently, the brain tissues were dried in a desiccating oven at 105°C to obtain the dry weight. The brain water content was calculated according to the previous described [30].

2.5. Cell Culture and Treatment. PC12 cells procured from the Culture Collection of the Chinese Academy of Science (Shanghai, China) were cultured in DMEM containing 10% fetal bovine serum and 1% penicillin/streptomycin. Oxygen and glucose deprivation/reperfusion (OGD/R) was established by culturing the cells in glucose-free DMEM and hypoxic conditions with $95\%N_2/5\%CO_2$. After 2 h of hypoxia, the cells were transferred back to full culture medium under normal atmosphere and incubated for 24 h. At 3h before OGD/R, rIL-22 (100 ng/mL) was administrated. To knockdown JAK2 and STAT3 expression, PC12 cells were transfected with si-JAK2 and si-STAT3, respectively, using Lipofectamine 2000 according to the manufacturer's recommendation.

2.6. ELISA. After 24 h of reperfusion, blood specimens were obtained from mice and centrifuged to separate the serum. The levels of IL-1β, monocyte chemotactic protein- (MCP-) 1, and tumor necrosis factor- (TNF-) α were measured by ELISA kits (R&D Systems, USA) according to the manufacturer's instructions.

2.7. Oxidative Stress Detection. After 24 h of reperfusion, the brain tissues were rapidly removed and prepared as homogenates, and then, the supernatants were collected. For the cells, PC12 cells were harvested and lysed, and then, the supernatants were collected. The activity of total superoxide dismutase (SOD) and glutathione (GSH) and the concentration of malondialdehyde (MDA) were measured by commercial assay kits (Beyotime Biotechnology, China) according to the manufacturer's instructions.

2.8. Apoptosis Assay. Cell apoptosis was measured by a terminal deoxynucleotidyl transferase-mediated dUTP nick end labeling (TUNEL) assay kit, as previously described [31]. Briefly, the slices were incubated with TUNEL reagents, and DAPI solution was prepared according to the manufacturer's

TABLE 1: Primer sequences for RT-PCR assays.

Gene	Species		Sequence ($5'$-$3'$)
IL-1β	Mouse	Forward	GGGCCTCAAAGGAAAGAATC
		Reverse	TACCAGTTGGGGAACTCTGC
IL-1β	Rat	Forward	GTGCTGTCTGACCCATGTGA
		Reverse	CACAGGGATTTTGTCGTTGCT
MCP-1	Mouse	Forward	GAGGTCACTCCTATCCTCTGG
		Reverse	GCCATTTCCTCCGACTTTTCTC
MCP-1	Rat	Forward	AGCATCCACGTGCTGTCTC
		Reverse	GATCATCTTGCCAGTGAATGAG
TNF-α	Mouse	Forward	CCCAGGGACCTCTCTCTAATC
		Reverse	ATGGGCTACAGGCTTGTCACT
TNF-α	Rat	Forward	CTACTCCCAGGTTCTCTTCAA
		Reverse	GCTGACTTTCTCCTGGTATGA
β-Actin	Mouse	Forward	TATTGGCAACGAGCGGTTCC
		Reverse	GGCATAGAGGTCTTTACGGATGT
β-Actin	Rat	Forward	CAAGAAGGTGGTGAAGCAG
		Reverse	AAAGGTGGAAGAATGGGAG

instructions. The number and ratio of TUNEL-positive cells were calculated based on the apoptosis index evaluated by an investigator blinded to the experiment.

2.9. Quantitative Real-Time RT-PCR. Total RNA was extracted from the ischemic hemisphere and PC12 cells using a TRIzol reagent and then reverse transcribed into cDNA according to the manufacturer's protocol. Real-time PCR analysis was performed using a LightCycler 480 qPCR System. The relative expression of target genes was normalized against β-actin mRNA. The primer sequences are presented in Table 1.

2.10. Western Blotting. Protein was extracted from the ischemic hemisphere and PC12 cells and then separated using SDS-PAGE. The proteins were transferred onto an Immobilon-P membrane (Millipore, USA). The membranes were incubated with primary antibodies against Bax, Bcl-2, p-JAK2, JAK2, p-STAT3, STAT3, and β-actin, followed by incubation with the secondary antibody. Finally, proteins on the membranes were detected using an Odyssey infrared imaging system (LI-COR, USA), and the protein expression levels were normalized to that of β-actin.

2.11. Statistical Analysis. Statistical analyses were performed using SPSS software. Normally distributed data are expressed as the mean ± standard deviation (SD). One-way analysis of variance (ANOVA) was used for comparisons among multiple groups, and when the differences were statistically significant, a post hoc Tukey test was carried out. Nonnormally distributed data are expressed as the median and quartiles. The Kruskal-Wallis H test was used for comparisons among multiple groups, and when the differences were statistically significant, the Mann-Whitney U test was carried out followed by Bonferroni correction. The Bonferroni correction is $\alpha' = 0.05/K$, where K is the number of comparisons.

P values less than 0.05 were considered statistically significant.

3. Results

3.1. IL-22 Treatment Ameliorated Cerebral I/R Injury. After ischemia-reperfusion, significant cerebral infarction was observed in the MCAO group, but IL-22 treatment significantly decreased the infarct volume of mice (Figures 1(a) and 1(b)). In addition, IL-22 administration significantly ameliorated neurological deficits and brain water content after cerebral I/R injury (Figures 1(c) and 1(d)).

3.2. IL-22 Treatment Inhibited the Inflammatory Response after Cerebral I/R Injury. Compared with the sham group, serum levels of inflammatory cytokines, including IL-1β, MCP-1, and TNF-α, in the MCAO group were significantly increased, while IL-22 treatment reduced the serum levels of these cytokines (Figures 2(a)–2(c)). Furthermore, IL-22 treatment also decreased the mRNA expression of IL-1β, MCP-1, and TNF-α in the ischemic cerebral cortex (Figures 2(d)–2(f)).

3.3. IL-22 Treatment Attenuated Oxidative Stress and Neuronal Apoptosis after Cerebral I/R Injury. Compared with the sham group, the activities of SOD and GSH in the MCAO group were significantly decreased and the levels of MDA were significantly increased after cerebral I/R injury (Figures 3(a)–3(c)). Interestingly, the activities of SOD and GSH in the brain tissues were significantly increased, and the levels of MDA were significantly reduced in the rIL-22 group compared with those in the MCAO group (Figures 3(a)–3(c)). The TUNEL staining results also showed that IL-22 treatment significantly decreased neuronal apoptosis after cerebral I/R (Figure 3(d)).
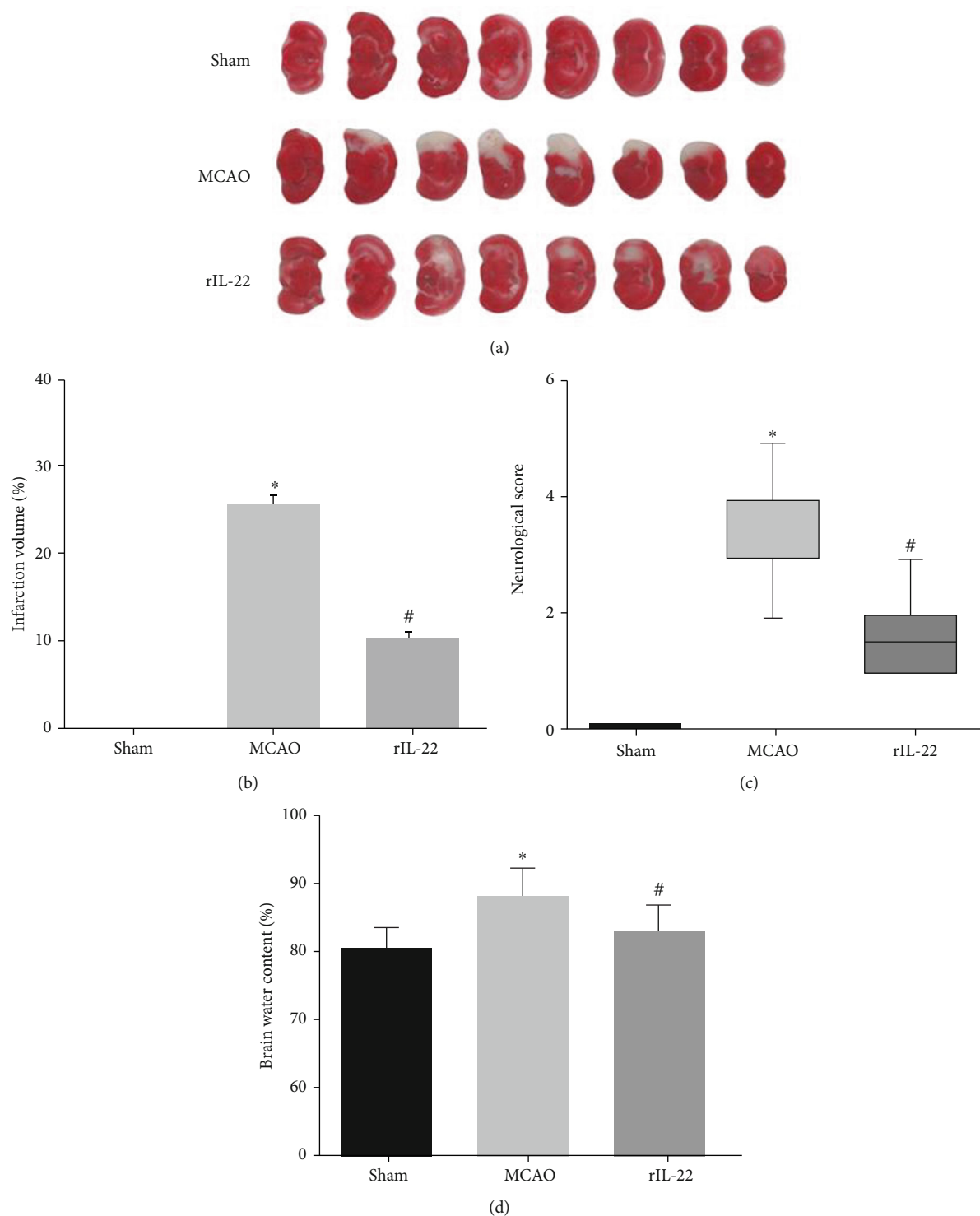
(a)

(b)

(c)

(d)

FIGURE 1: IL-22 treatment ameliorated cerebral I/R injury. (a) Representative sections of TTC staining in each group ($n = 6$). (b) Quantification of infarct volume in each group ($n = 6$). (c) Neurological deficits were assessed in each group ($n = 8$). (d) Brain water content was calculated in each group ($n = 6$). $^*P < 0.05$ vs sham group; $^\#P < 0.05$ vs MCAO group.

3.4. IL-22 Treatment Inhibited OGD/R-Induced Inflammation and Oxidative Stress. Our results showed that IL-22 treatment significantly decreased the mRNA expression of IL-1β, MCP-1, and TNF-α after OGD/R (Figures 4(a)–4(c)). In addition, IL-22 treatment significantly increased the activities of SOD and

GSH and reduced the levels of MDA compared with the OGD/R group (Figures 4(d)–4(f)).

3.5. IL-22 Treatment Attenuated OGD/R-Induced Neuronal Apoptosis. The TUNEL staining results showed that the
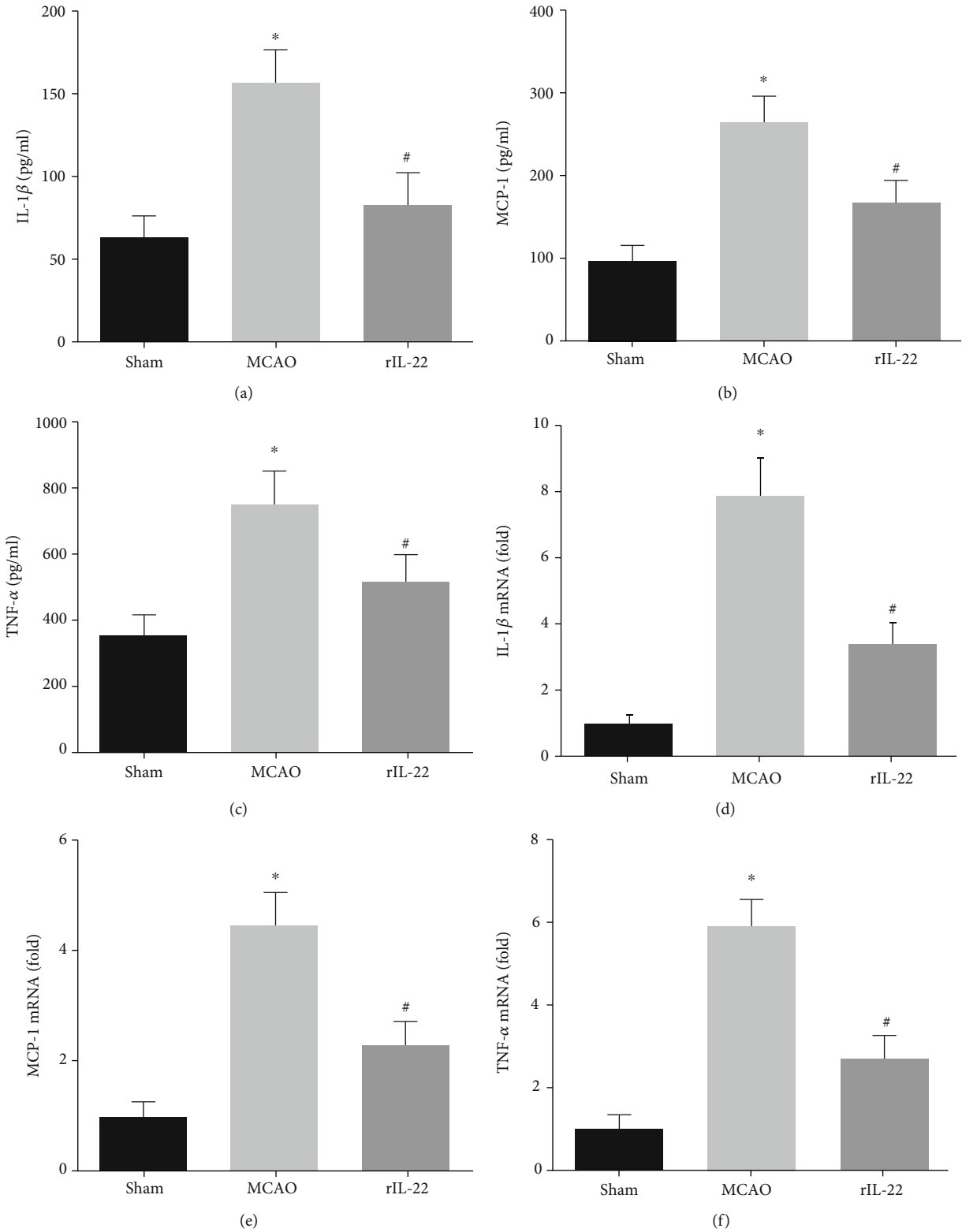
Figure 2: IL-22 treatment inhibited the inflammatory response after cerebral I/R injury. Serum levels of IL-1β (a), MCP-1 (b), and TNF-α (c) were measured by ELISA ($n = 8$). The mRNA expression of IL-1β (d), MCP-1 (e), and TNF-α (f) was detected in brain tissues ($n = 8$). *$P < 0.05$ vs. sham group; #$P < 0.05$ vs. MCAO group.

(a)

(b)

(c)

(d)
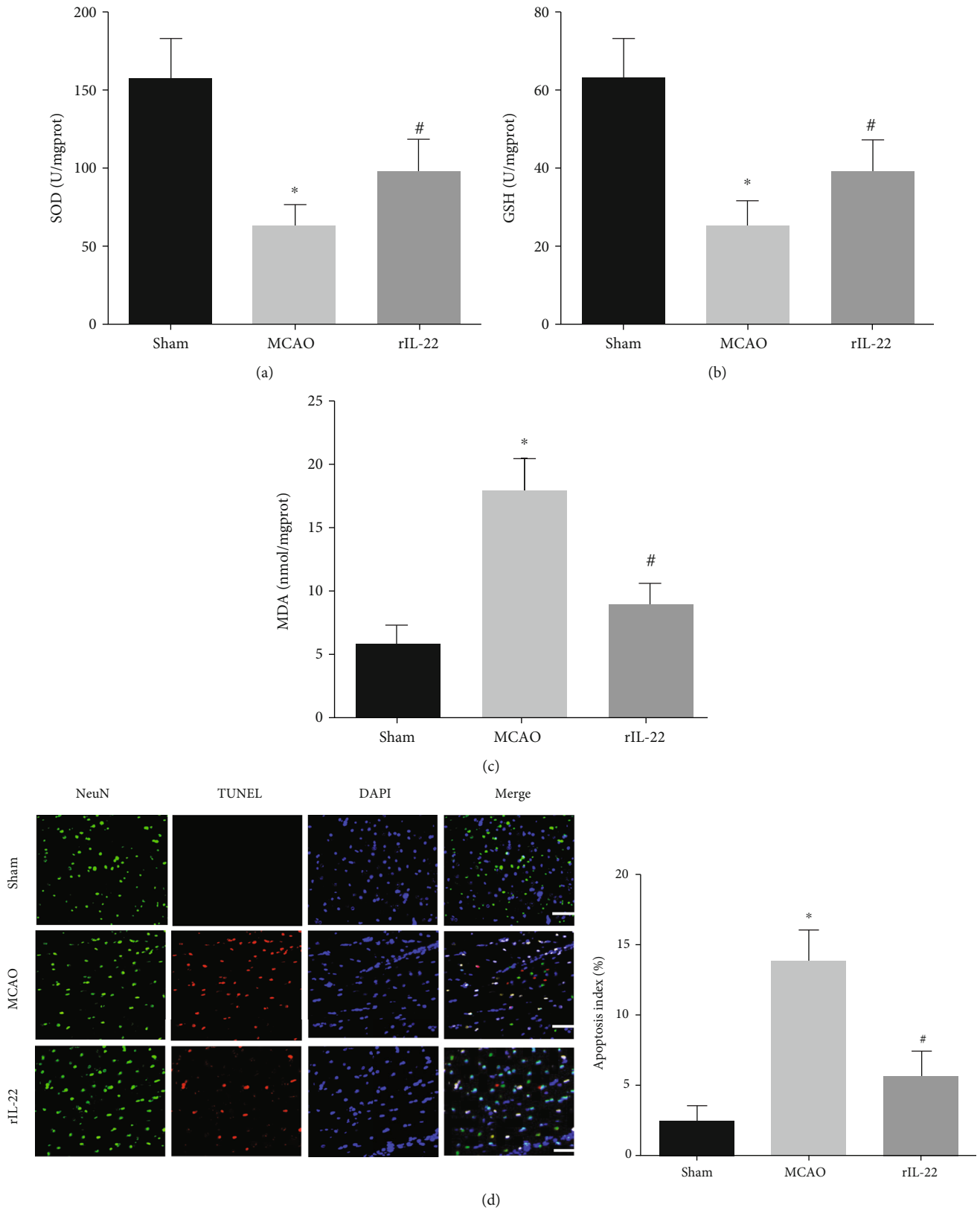
Figure 3: IL-22 treatment attenuated oxidative stress and neuronal apoptosis after cerebral I/R injury. The levels of SOD (a), GSH (b), and MDA (c) were detected in brain tissues ($n = 6$). (d) Neuronal apoptosis was detected by TUNEL staining combined with immunostaining for NeuN ($n = 5$, scale bar = 75 μm). $^{*}P < 0.05$ vs. sham group; $^{\#}P < 0.05$ vs. MCAO group.

Figure 4: IL-22 treatment inhibited OGD/R-induced inflammation and oxidative stress. The mRNA expression of IL-1β (a), MCP-1 (b), and TNF-α (c) was detected in PC12 cells ($n = 6$). The levels of SOD (d), GSH (e), and MDA (f) were detected in PC12 cells ($n = 6$). $^*P < 0.05$ vs. PBS group; $^\#P < 0.05$ vs. OGD/R group.

(a)

(b)

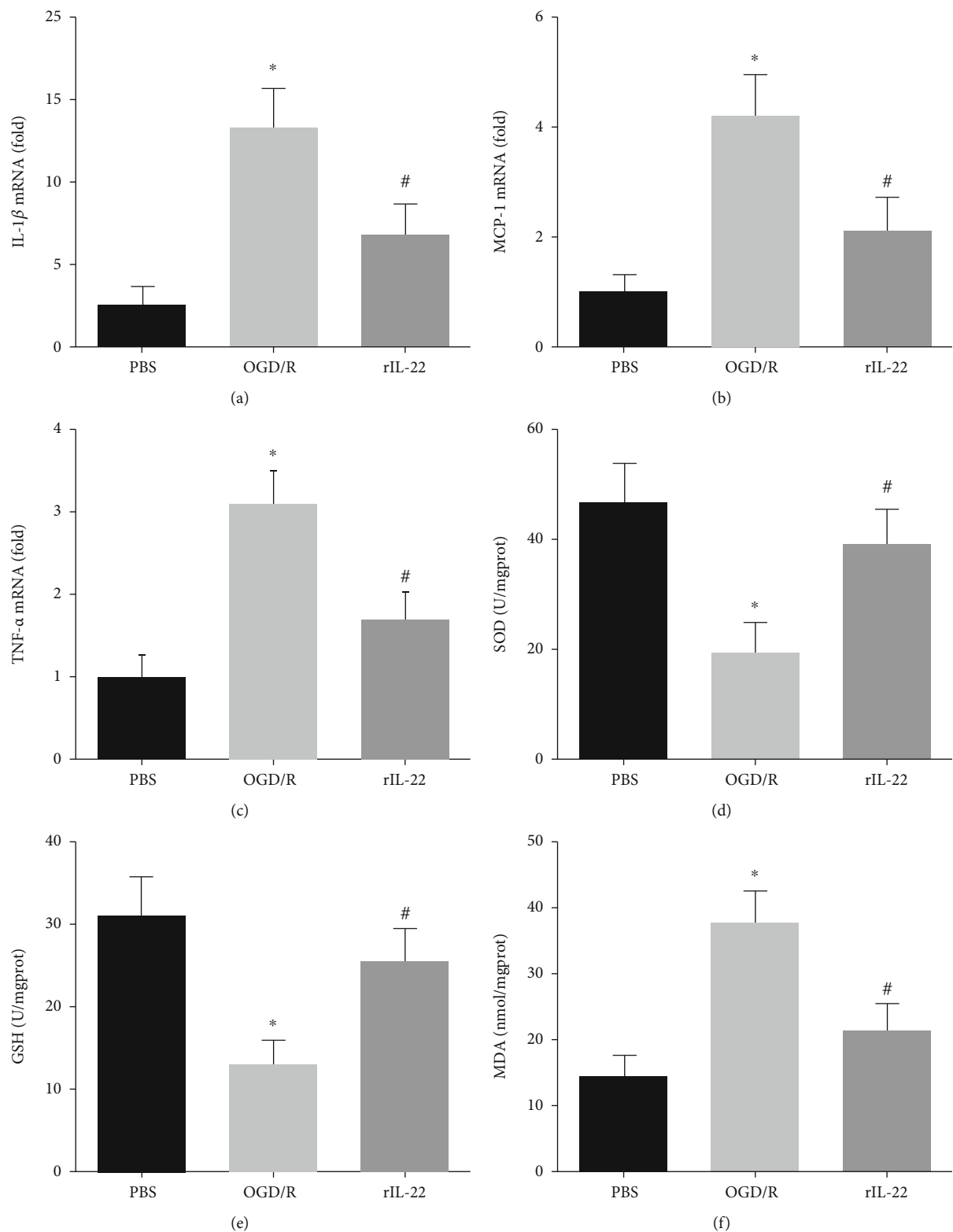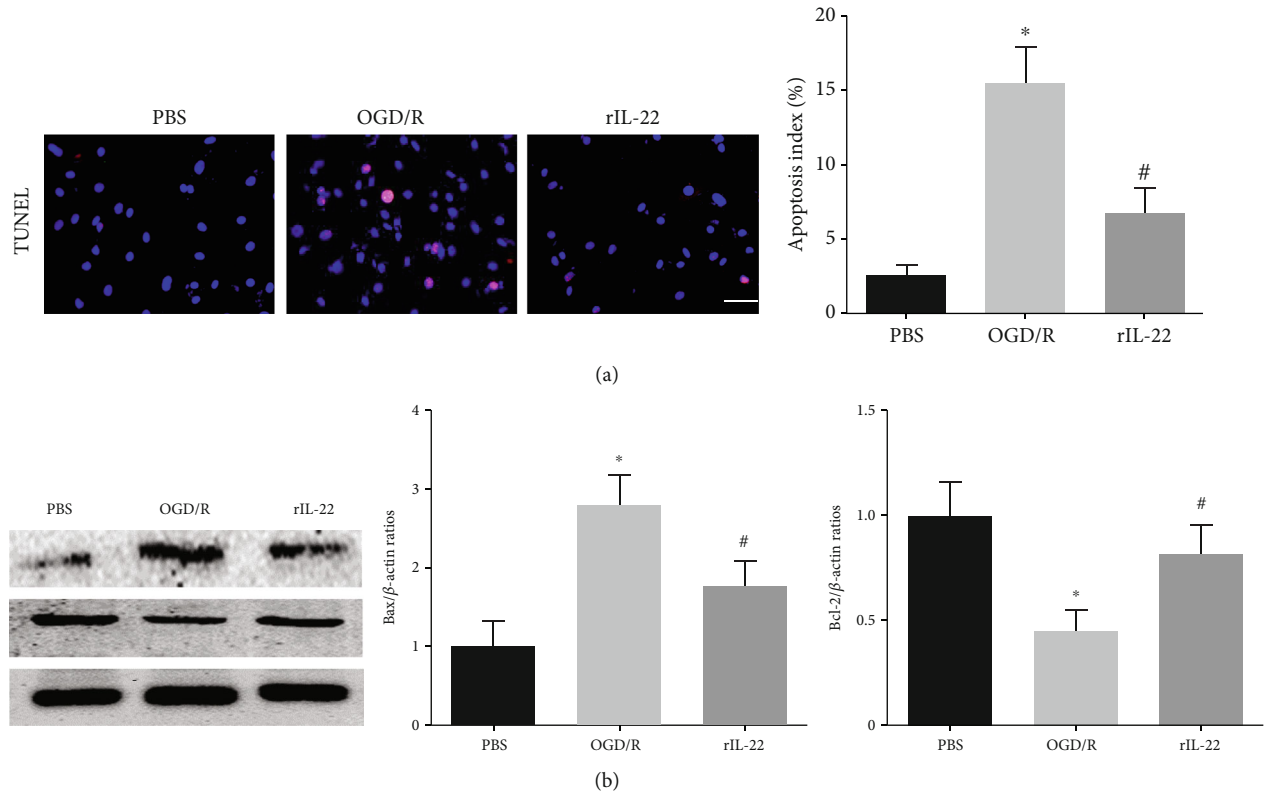FIGURE 5: IL-22 treatment attenuated OGD/R-induced neuronal apoptosis. (a) Neuronal apoptosis was detected by TUNEL staining ($n = 5$, scale bar = 50 μm). (b) The expression of Bax, Bcl-2, and β-actin was detected by western blotting ($n = 4$). $^*P < 0.05$ vs. PBS group; $^\#P < 0.05$ vs. OGD/R group.

apoptotic index in the OGD/R group was significantly lower than that in the PBS group, while IL-22 treatment significantly diminished OGD-induced cell apoptosis (Figure 5(a)). In addition, IL-22 treatment significantly attenuated the restored Bcl-2 expression and reduced Bax expression after OGD/R insult (Figure 5(b)).

3.6. IL-22 Treatment Activated the JAK2/STAT3 Signaling Pathway. Our results showed that the phosphorylation levels of JAK2 and STAT3 in the MCAO group were significantly higher than those in the sham group, and IL-22 treatment further increased JAK2 and STAT3 phosphorylation levels (Figure 6(a)). In addition, our results also showed that IL-22 treatment upregulated JAK2 and STAT3 phosphorylation levels in PC12 cells after OGD/R insult (Figure 6(b)).

3.7. JAK2 and STAT3 Knockdown Abolished IL-22-Mediated Neuroprotection. To further confirm the effect of the JAK2/STAT3 signaling pathway in IL-22-mediated neuroprotection, transfection with si-JAK2 and si-STAT3 was performed to knock down JAK2 and STAT3 expression in vitro, respectively. The results showed that JAK2 and STAT3 knockdown abolished the IL-22-mediated anti-inflammatory effects by increasing IL-1β, MCP-1, and TNF-α mRNA expression (Figures 7(a)–7(c)). In addition, JAK2 and STAT3 knockdown also attenuated IL-22-mediated antioxidative stress and antiapoptotic effects (Figures 7(d)–7(g)). The above results revealed

that the JAK2/STAT3 pathway plays a central role in IL-22-mediated neuroprotective effects.

4. Discussion

In the current study, we investigated the protective effect of IL-22 against cerebral I/R injury. We provided direct evidence that IL-22 treatment decreased infarct size, neurological deficits, and brain water content in mice subjected to cerebral I/R injury. IL-22 treatment remarkably attenuated the inflammatory response, oxidative stress, and neuronal apoptosis after cerebral I/R injury. In addition, IL-22 treatment decreased the inflammatory response, oxidative stress, and apoptosis of PC12 cells after OGD/R insult. Moreover, IL-22 treatment significantly increased JAK2 and STAT3 phosphorylation levels in mice and PC12 cells, and STAT3 knockdown abolished the IL-22-mediated neuroprotective function. These findings suggest that IL-22 could be exploited as a potential therapeutic agent for ischemic stroke and cerebral I/R injury.

Based on similarities in structure and receptor subunits, the IL-10 family comprises six members, including IL-10, IL-19, IL-20, IL-22, IL-24, and IL-26 [32–34]. As an anti-inflammatory cytokine, the neuroprotective effect of IL-10 on cerebral I/R injury has been identified in numerous studies [35, 36]. In addition, IL-19 administration also reduced ischemia-induced brain infarct and neurological deficits in mice after experimental ischemic stroke, indicating that IL-19
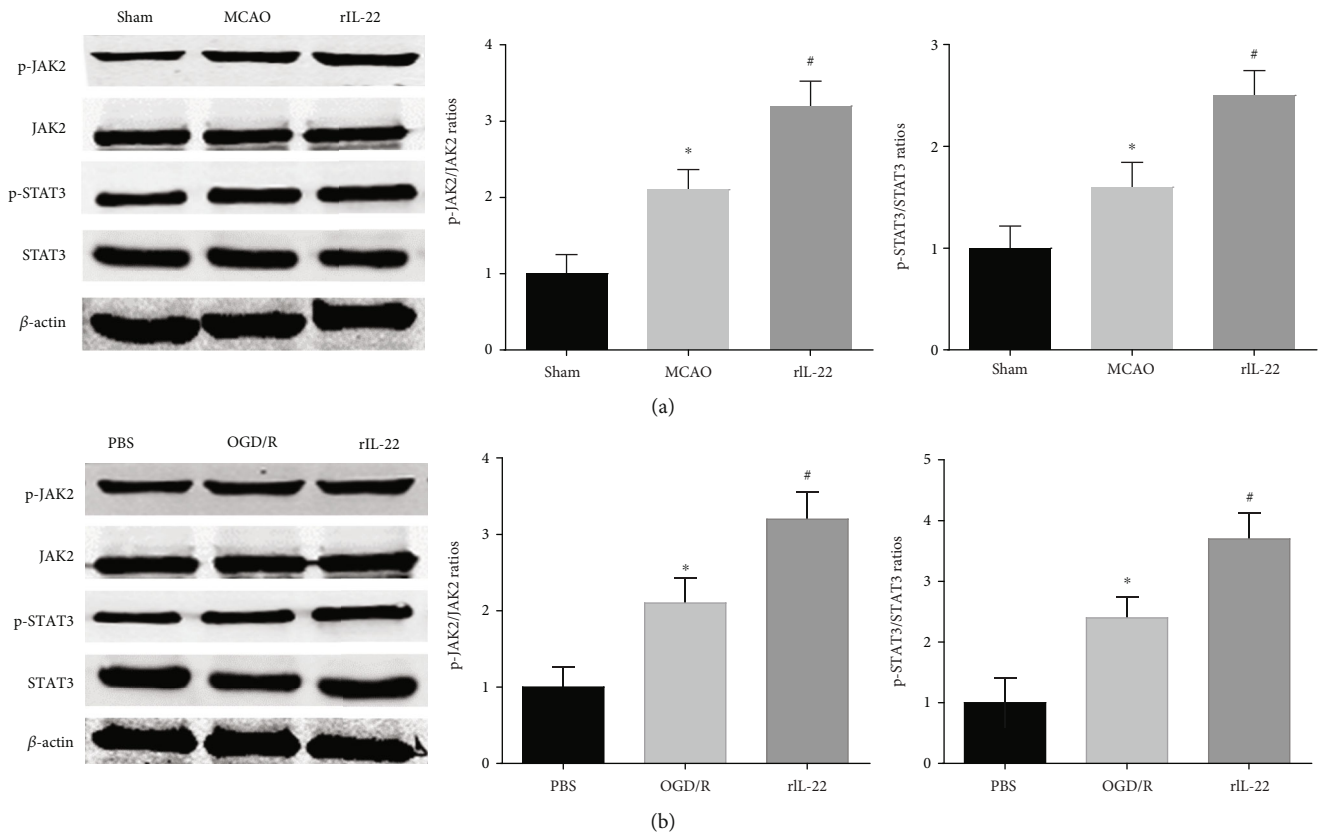
FIGURE 6: IL-22 treatment activated the JAK2/STAT3 signaling pathway. (a) The expression of p-JAK2, JAK2, p-STAT3, STAT3, and β-actin in the brain was detected by western blotting ($n = 4$). (b) The expression of p-JAK2, JAK2, p-STAT3, STAT3, and β-actin in PC12 cells was detected by western blotting ($n = 4$). $^*P < 0.05$ vs. the sham or PBS group; $^\#P < 0.05$ vs. the MCAO or OGD/R group.

is a novel therapeutic target for cerebral I/R injury [37]. However, IL-20 expression was upregulated in the serum and brain tissue of rats after cerebral I/R, and anti-IL-20 neutralizing antibody administration ameliorated MCAO-induced brain infarction in rats [38]. IL-22 was first identified as a product of CD4+ T cell subsets, and subsequent studies demonstrated that IL-22 is also secreted by macrophage, natural killer cells, and natural killer T cells [24, 39]. Previous studies reported that IL-22 was expressed in human brain tissue and mouse brain, and IL-22 treatment protected nutriment-deprived astrocytes from cell death [40, 41]. Liu et al. also reported that IL-22 treatment significantly inhibited serum starvation-induced PC12 cell death, indicating that IL-22 may confer a neuroprotective function [42].

The results showed that rIL-22 administered in advance significantly decreased the infarct volume and ameliorated neurological deficits and brain water content after cerebral I/R injury in mice. In addition, IL-22 treatment also diminished OGD/R-induced neuronal injury and apoptosis in vitro. These findings demonstrated that IL-22 exerts a neuroprotective effect on cerebral ischemic injury.

The inflammatory response plays a pivotal role in the pathophysiology of I/R-induced cerebral injury. After stroke, the interruption and reperfusion of blood flow in brain tissue trigger inflammatory cell infiltration and cause a robust inflammatory response, which induces neuronal apoptosis and death [43, 44]. Multiple inflammatory-related cytokines

are released in ischemic brain injury and participate in the damage and repair process of brain tissue, including ILs, TNF, interferon, and chemokines [45, 46]. In addition, numerous data suggest that the inflammatory response is closely related to oxidative stress and aggravating I/R-induced cerebral injury [47, 48]. Thus, it is clear that therapeutic drugs targeting the inflammatory response and oxidative stress can be very effective in improving cerebral I/R injury. Previous research has shown that IL-22 is an inflammation-related cytokine and has anti-inflammatory and antioxidative stress effects. Thus, we investigated whether IL-22 affects the inflammatory response and oxidative stress in MCAO-induced cerebral I/R injury.

Our results showed that serum levels of inflammatory cytokines, including IL-1β, MCP-1, and TNF-α, in the MCAO group were significantly higher than those in the sham group, while IL-22 treatment significantly reduced the serum levels of these cytokines. In addition, IL-22 treatment also decreased the mRNA expression of IL-1β, MCP-1, and TNF-α in brain tissue after cerebral I/R injury. To assess the effects of IL-22 on cerebral I/R-induced oxidative stress, we measured the SOD and GSH activities and MDA contents in brain tissues. The results showed that the activities of SOD and GSH in the brain tissues were significantly increased and the levels of MDA were significantly reduced in the rIL-22 group compared with those in the MCAO group.
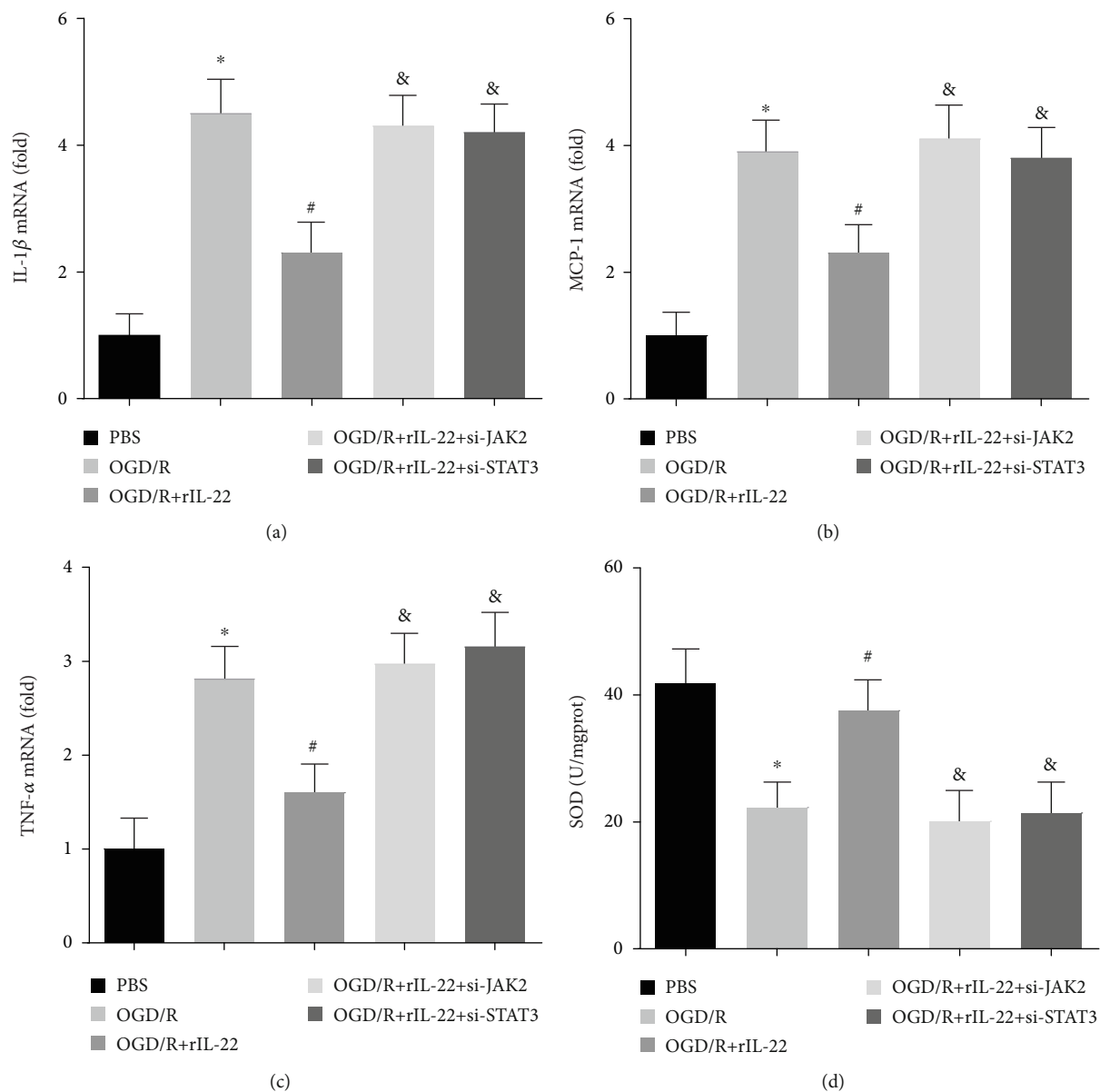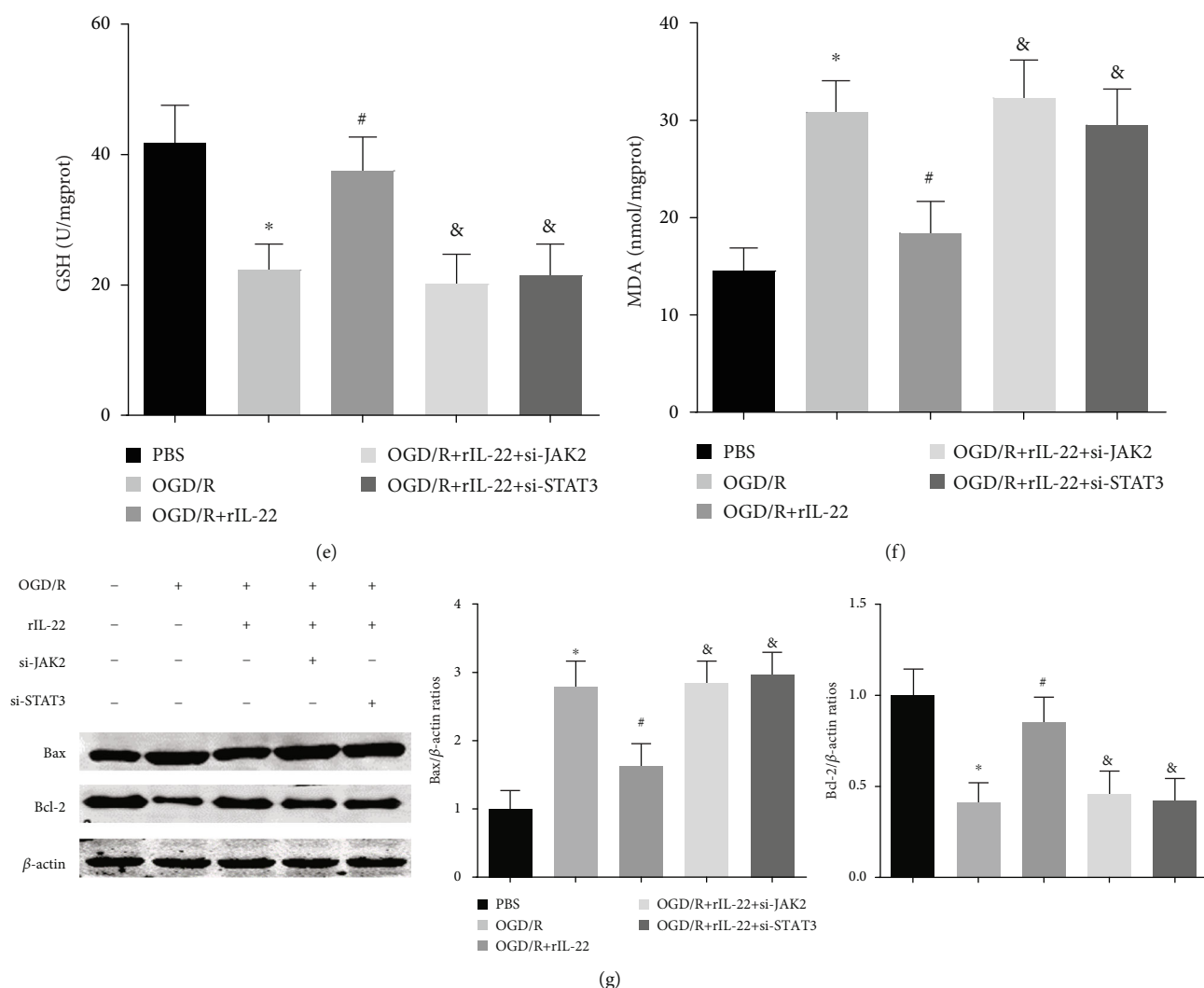
(a)

(b)

(c)

(d)

FIGURE 7: Continued.

(e)

(f)

(g)

Figure 7: JAK2 and STAT3 knockdown abolished IL-22-mediated neuroprotection. The mRNA expression of IL-1β (a), MCP-1 (b), and TNF-α (c) was detected in PC12 cells ($n = 6$). The levels of SOD (d), GSH (e), and MDA (f) were detected in PC12 cells ($n = 6$). (g) The expression of Bax, Bcl-2, and β-actin was detected by western blotting ($n = 4$). *$P < 0.05$ vs. PBS group; #$P < 0.05$ vs. OGD/R group; &$P < 0.05$ vs. OGD/R+rIL-22 group.

Signaling through the JAK/STAT pathway is important for the progression of neurological diseases, including stroke, traumatic brain injury, status epilepticus, brain tumors, and neurodegenerative diseases [49, 50]. Many lines of evidence have indicated that JAK2/STAT3 signaling is activated in the early stage of cerebral ischemia and mediates oxidative stress, the inflammatory response, and neuronal apoptosis [49, 51]. Kinouchi et al. reported that pioglitazone protects against cerebral I/R injury by activating the JAK2/STAT3 signaling pathway [52]. Liu et al. reported that diosmin inhibits neuronal apoptosis by activating the JAK2/STAT3 signaling pathway after cerebral ischemia in mice [53]. Accumulating evidence suggests that JAK2/STAT3 is a major downstream signal of IL-22 and mediates its hepatoprotective and cardioprotective functions [25, 39].

In the current study, we investigated the role of IL-22 treatment in JAK2/STAT3 signaling after cerebral I/R. The results showed that the phosphorylation levels of JAK2 and STAT3 were upregulated in mice after cerebral I/R injury

and in PC12 cells following OGD/R. In addition, IL-22 treatment further increased JAK2 and STAT3 phosphorylation levels, and STAT3 knockdown abolished the IL-22-mediated neuroprotective function. These findings indicate that the neuroprotective actions of IL-22 are related to the JAK2/STAT3 signaling pathway.

Over the last decade, evidence supporting combination therapies has been obtained from a variety of studies in many types of animal models [54, 55]. The combination of thrombolysis and neuroprotection has been considered a promising approach for the treatment of acute ischemic stroke [55, 56]. Tissue plasminogen activator (tPA) is the only treatment approved by the USA FDA for acute ischemic stroke; it dissolves the obstructive clot to restore cerebral blood flow [57]. Neuroprotective agents attenuate the inflammatory response and suppress molecules that mediate thrombosis and blood-brain barrier disruption induced by ischemia such that the benefits of tPA may be extended [55, 56]. Our study shows that IL-22 may be a promising neuroprotective agent;

however, the combined effect of IL-22 and tPA is still unclear and will be the focus of our next study.

In conclusion, our findings provide preliminary evidence demonstrating the roles of IL-22 in cerebral I/R injury. IL-22 treatment prevented I/R-induced cerebral injury and neurological deficits by alleviating the inflammatory response, oxidative stress, and neuronal apoptosis. Our data indicate that IL-22 may serve as an attractive therapeutic target for treating ischemic stroke and cerebral I/R injury.

Data Availability

The datasets generated and/or analyzed during the current study are available from the corresponding author on reasonable request in compliance with ethical standards.

Conflicts of Interest

No conflicts of interests are declared by the authors.

Authors' Contributions

Chaoshi Niu was involved in the design and execution of experiments, data analysis, and manuscript writing. Yongfei Dong and Chengyun Hu were involved in the design of the study, the execution of experiments, data analysis, and manuscript writing. Chunxia Huang, Jie Gao, Wanxiang Niu, Di Wang, and Yang Wang were all involved in the execution of experiments and data analysis. All authors provided final approval of the version to be submitted. Yongfei Dong and Chengyun Hu contributed equally to this work.

Acknowledgments

References

[1] C. O. Johnson, M. Nguyen, G. A. Roth et al., "Global, regional, and national burden of stroke, 1990-2016: a systematic analysis for the Global Burden of Disease Study 2016," *The Lancet Neurology*, vol. 18, no. 5, pp. 439–458, 2019.

[2] P. B. Gorelick, "The global burden of stroke: persistent and disabling," *The Lancet Neurology*, vol. 18, no. 5, pp. 417-418, 2019.

[3] H. Amani, E. Mostafavi, M. R. Alebouyeh et al., "Would colloidal gold nanocarriers present an effective diagnosis or treatment for ischemic stroke?," *International Journal of Nanomedicine*, vol. 14, pp. 8013–8031, 2019.

[4] G. Xiao, M. Lyu, Y. Wang et al., "Ginkgo flavonol glycosides or ginkgolides tend to differentially protect myocardial or cerebral ischemia-reperfusion injury via regulation of TWEAK-Fn14 signaling in heart and brain," *Frontiers in Pharmacology*, vol. 10, p. 735, 2019.

[5] M. S. Khan, A. Khan, S. Ahmad et al., "Inhibition of JNK alleviates chronic hypoperfusion-related ischemia induces oxidative stress and brain degeneration via Nrf2/HO-1 and NF-κB signaling," *Oxidative Medicine and Cellular Longevity*, vol. 2020, Article ID 5291852, 18 pages, 2020.

[6] F. Wu, Y. Ling, L. Yang, X. Cheng, Q. Dong, and W. Cao, "High level of serum tissue kallikrein is associated with favorable outcome in acute ischemic stroke patients," *Disease Markers*, vol. 2019, Article ID 5289715, 6 pages, 2019.

[7] Y. Cao, C. Cui, H. Zhao et al., "Plasma osteoprotegerin correlates with stroke severity and the occurrence of microembolic signals in patients with acute ischemic stroke," *Disease Markers*, vol. 2019, Article ID 3090364, 7 pages, 2019.

[8] W. Zhang, J. Song, W. Li et al., "Salvianolic acid D alleviates cerebral ischemia-reperfusion injury by suppressing the cytoplasmic translocation and release of HMGB1-triggered NF-κB activation to inhibit inflammatory response," *Mediators of Inflammation*, vol. 2020, Article ID 9049614, 15 pages, 2020.

[9] J. D. Bernstock, L. Peruzzotti-Jametti, T. Leonardi et al., "SUMOylation promotes survival and integration of neural stem cell grafts in ischemic stroke," *eBioMedicine*, vol. 42, pp. 214–224, 2019.

[10] W. Geng, L. Cai, K. Han et al., "Electroacupuncture pretreatment alleviates cerebral ischemia-reperfusion injury by increasing GSK-3β phosphorylation level via adenosine A1 receptor," *BioMed Research International*, vol. 2020, Article ID 6848450, 9 pages, 2020.

[11] Y. Huang, Z. Liu, F. Tan, Z. Hu, and M. Lu, "Effects of the insulted neuronal cells-derived extracellular vesicles on the survival of umbilical cord-derived mesenchymal stem cells following cerebral ischemia/reperfusion injury," *Oxidative Medicine and Cellular Longevity*, vol. 2020, Article ID 9768713, 26 pages, 2020.

[12] J. Zeng, L. Zhu, J. Liu et al., "Metformin protects against oxidative stress injury induced by ischemia/reperfusion via regulation of the lncRNA-H19/miR-148a-3p/Rock2 axis," *Oxidative Medicine and Cellular Longevity*, vol. 2019, Article ID 8768327, 18 pages, 2019.

[13] B. Zhang, H. X. Zhang, S. T. Shi et al., "Interleukin-11 treatment protected against cerebral ischemia/reperfusion injury," *Biomedicine & Pharmacotherapy*, vol. 115, article ???, 2019.

[14] B. D. Semple, L. K. Dill, and T. J. O'Brien, "Immune challenges and seizures: how do early life insults influence epileptogenesis?," *Frontiers in Pharmacology*, vol. 11, p. 2, 2020.

[15] J. Liu, Y. Xing, Y. Gao, and C. Zhou, "Changes in serum interleukin-33 levels in patients with acute cerebral infarction," *Journal of Clinical Neuroscience*, vol. 21, no. 2, pp. 298–300, 2014.

[16] C. J. Smith, S. Hulme, A. Vail et al., "SCIL-STROKE (subcutaneous interleukin-1 receptor antagonist in ischemic stroke): a randomized controlled phase 2 trial," *Stroke*, vol. 49, no. 5, pp. 1210–1216, 2018.

[17] C. Xu, H. Zhu, R. Shen, Q. Feng, H. Zhou, and Z. Zhao, "IL-35 is a protective immunomodulator in brain ischemic injury in mice," *Neurochemical Research*, vol. 43, no. 7, pp. 1454–1463, 2018.

[18] C. Liu, X. Xu, C. Huang, D. Shang, L. Zhang, and Y. Wang, "Inhibition of IL-32 expression ameliorates cerebral ischemia-reperfusion injury via the NOD/MAPK/NF-κB signaling pathway," *Journal of Molecular Neuroscience*, vol. 70, no. 11, pp. 1713–1727, 2020.

[19] M. H. Xie, S. Aggarwal, W. H. Ho et al., "Interleukin (IL)-22, a novel human cytokine that signals through the interferon receptor-related proteins CRF2-4 and IL-22R∗," *The Journal of Biological Chemistry*, vol. 275, no. 40, pp. 31335–31339, 2000.

[20] J. A. Dudakov, A. M. Hanash, and M. R. van den Brink, "Interleukin-22: immunobiology and pathology," *Annual Review of Immunology*, vol. 33, no. 1, pp. 747–785, 2015.

[21] M. Weidenbusch, S. Rodler, and H. J. Anders, "Interleukin-22 in kidney injury and regeneration," *American Journal of Physiology. Renal Physiology*, vol. 308, no. 10, pp. F1041–F1046, 2015.

[22] Y. Liu, V. K. Verma, H. Malhi et al., "Lipopolysaccharide downregulates macrophage-derived IL-22 to modulate alcohol-induced hepatocyte cell death," *American Journal of Physiology. Cell Physiology*, vol. 313, no. 3, pp. C305–C313, 2017.

[23] M. Hu, S. Yang, L. Yang, Y. Cheng, and H. Zhang, "Interleukin-22 alleviated palmitate-induced endoplasmic reticulum stress in INS-1 cells through activation of autophagy," *PLoS One*, vol. 11, article e146818, 2016.

[24] L. Shi, Q. Ji, L. Liu et al., "IL-22 produced by Th22 cells aggravates atherosclerosis development in ApoE−/−mice by enhancing DC-induced Th17 cell proliferation," *Journal of Cellular and Molecular Medicine*, vol. 24, no. 5, pp. 3064–3078, 2020.

[25] J. Takahashi, M. Yamamoto, H. Yasukawa et al., "Interleukin-22 directly activates myocardial STAT3 (signal transducer and activator of transcription-3) signaling pathway and prevents myocardial ischemia reperfusion injury," *Journal of the American Heart Association*, vol. 9, p. e14814, 2020.

[26] M. J. Xu, D. Feng, H. Wang, Y. Guan, X. Yan, and B. Gao, "IL-22 ameliorates renal ischemia-reperfusion injury by targeting proximal tubule epithelium," *Journal of the American Society of Nephrology*, vol. 25, no. 5, pp. 967–977, 2014.

[27] X. Guan, Y. Wang, G. Kai et al., "Cerebrolysin ameliorates focal cerebral ischemia injury through neuroinflammatory inhibition via CREB/PGC-1α pathway," *Frontiers in Pharmacology*, vol. 10, p. 1245, 2019.

[28] E. Z. Longa, P. R. Weinstein, S. Carlson, and R. Cummins, "Reversible middle cerebral artery occlusion without craniectomy in rats," *Stroke*, vol. 20, no. 1, pp. 84–91, 1989.

[29] J. Li, K. Zhang, Q. Zhang et al., "PPAR-γ mediates Ta-VNS-induced angiogenesis and subsequent functional recovery after experimental stroke in rats," *BioMed Research International*, vol. 2020, Article ID 8163789, 12 pages, 2020.

[30] C. Tang, Y. Hu, H. Lyu et al., "Neuroprotective effects of 1-O-hexyl-2,3,5-trimethylhydroquinone on ischaemia/reperfusion-induced neuronal injury by activating the Nrf2/HO-1 pathway," *Journal of Cellular and Molecular Medicine*, vol. 24, no. 18, pp. 10468–10477, 2020.

[31] L. Jiang, Y. Gong, Y. Hu et al., "Peroxiredoxin-1 overexpression attenuates doxorubicin-induced cardiotoxicity by inhibiting oxidative stress and cardiomyocyte apoptosis," *Oxidative Medicine and Cellular Longevity*, vol. 2020, Article ID 2405135, 11 pages, 2020.

[32] A. R. Burmeister and I. Marriott, "The interleukin-10 family of cytokines and their role in the CNS," *Frontiers in Cellular Neuroscience*, vol. 12, p. 458, 2018.

[33] E. Sziksz, D. Pap, R. Lippai et al., "Fibrosis related inflammatory mediators: role of the IL-10 cytokine family," *Mediators of Inflammation*, vol. 2015, Article ID 764641, 15 pages, 2015.

[34] M. Mocan, L. D. Mocan Hognogi, F. P. Anton et al., "Biomarkers of inflammation in left ventricular diastolic dysfunction," *Disease Markers*, vol. 2019, Article ID 7583690, 14 pages, 2019.

[35] M. Nakajima, C. Nito, K. Sowa et al., "Mesenchymal stem cells overexpressing interleukin-10 promote neuroprotection in experimental acute ischemic stroke," *Molecular Therapy - Methods & Clinical Development*, vol. 6, pp. 102–111, 2017.

[36] M. Chen and Y. Yang, "A meta-analysis on associations of *IL-6* and *IL-10* polymorphisms with susceptibility to ischemic stroke," *Journal of Neuroimmunology*, vol. 335, article 577004, 2019.

[37] W. Xie, L. Fang, S. Gan, and H. Xuan, "Interleukin-19 alleviates brain injury by anti-inflammatory effects in a mice model of focal cerebral ischemia," *Brain Research*, vol. 1650, pp. 172–177, 2016.

[38] W. Y. Chen and M. S. Chang, "IL-20 is regulated by hypoxia-inducible factor and up-regulated after experimental ischemic stroke," *Journal of Immunology*, vol. 182, no. 8, pp. 5003–5012, 2009.

[39] X. Xiang, S. Hwang, D. Feng, V. H. Shah, and B. Gao, "Interleukin-22 in alcoholic hepatitis and beyond," *Hepatology International*, vol. 14, no. 5, pp. 667–676, 2020.

[40] G. Perriard, A. Mathias, L. Enz et al., "Interleukin-22 is increased in multiple sclerosis patients and targets astrocytes," *Journal of Neuroinflammation*, vol. 12, no. 1, p. 119, 2015.

[41] L. Dumoutier, J. Louahed, and J. C. Renauld, "Cloning and characterization of IL-10-related T cell-derived inducible factor (IL-TIF), a novel cytokine structurally related to IL-10 and inducible by IL-9," *Journal of Immunology*, vol. 164, no. 4, pp. 1814–1819, 2000.

[42] Y. Liu, W. Pan, S. Yang et al., "Interleukin-22 protects rat PC12 pheochromocytoma cells from serum deprivation-induced cell death," *Molecular and Cellular Biochemistry*, vol. 371, no. 1-2, pp. 137–146, 2012.

[43] G. Wang, B. Han, L. Shen et al., "Silencing of circular RNA HIPK2 in neural stem cells enhances functional recovery following ischaemic stroke," *eBioMedicine*, vol. 52, article 102660, 2020.

[44] J. Wang, J. Mao, R. Wang, S. Li, B. Wu, and Y. Yuan, "Kaempferol protects against cerebral ischemia reperfusion injury through intervening oxidative and inflammatory stress induced apoptosis," *Frontiers in Pharmacology*, vol. 11, p. 424, 2020.

[45] H. Pawluk, A. Woźniak, G. Grześk et al., "The role of selected pro-inflammatory cytokines in pathogenesis of ischemic stroke," *Clinical Interventions in Aging*, vol. 15, pp. 469–484, 2020.

[46] L. Zhang, C. Liu, C. Huang, X. Xu, and J. Teng, "miR-155 knockdown protects against cerebral ischemia and reperfusion injury by targeting MafB," *BioMed Research International*, vol. 2020, Article ID 6458204, 11 pages, 2020.

[47] J. Yu, W.-N. Wang, N. Matei et al., "Ezetimibe attenuates oxidative stress and neuroinflammation via the AMPK/Nrf2/TX-NIP pathway after MCAO in rats," *Oxidative Medicine and Cellular Longevity*, vol. 2020, Article ID 4717258, 14 pages, 2020.

[48] J. Wattanathorn, W. Ohnon, W. Thukhammee, S. Muchmapura, P. Wannanon, and T. Tong-Un, "Cerebroprotective effect against cerebral ischemia of the combined extract of Oryza sativa and Anethum graveolens in metabolic syndrome rats," *Oxidative Medicine and Cellular Longevity*, vol. 2019, Article ID 9658267, 19 pages, 2019.

[49] C. S. Nicolas, M. Amici, Z. A. Bortolotto et al., "The role of JAK-STAT signaling within the CNS," *JAK-STAT*, vol. 2, no. 1, article e22925, 2014.

[50] L. Li, L. Sun, Y. Qiu, W. Zhu, K. Hu, and J. Mao, "Protective effect of stachydrine against cerebral ischemia-reperfusion injury by reducing inflammation and apoptosis through P65 and JAK2/STAT3 signaling pathway," *Frontiers in Pharmacology*, vol. 11, p. 64, 2020.

[51] Z. Liang, G. Wu, C. Fan et al., "The emerging role of signal transducer and activator of transcription 3 in cerebral ischemic and hemorrhagic stroke," *Progress in Neurobiology*, vol. 137, pp. 1–16, 2016.

[52] T. Kinouchi, K. T. Kitazato, K. Shimada et al., "Activation of signal transducer and activator of transcription-3 by a peroxisome proliferator-activated receptor gamma agonist contributes to neuroprotection in the peri-infarct region after ischemia in oophorectomized rats," *Stroke*, vol. 43, no. 2, pp. 478–483, 2012.

[53] X. Liu, X. Zhang, J. Zhang et al., "Diosmin protects against cerebral ischemia/reperfusion injury through activating JAK2/STAT3 signal pathway in mice," *Neuroscience*, vol. 268, pp. 318–327, 2014.

[54] F. Poustchi, H. Amani, Z. Ahmadian et al., "Combination therapy of killing diseases by injectable hydrogels: from concept to medical applications," *Advanced Healthcare Materials*, vol. 10, no. 3, article e2001571, 2021.

[55] Y. Wang, Q. Li, J. Wang, Q. K. Zhuang, and Y. Y. Zhang, "Combination of thrombolytic therapy and neuroprotective therapy in acute ischemic stroke: is it important?," *European Review for Medical and Pharmacological Sciences*, vol. 19, no. 3, pp. 416–422, 2015.

[56] T. Fukuta, T. Asai, Y. Yanagida et al., "Combination therapy with liposomal neuroprotectants and tissue plasminogen activator for treatment of ischemic stroke," *The FASEB Journal*, vol. 31, no. 5, pp. 1879–1890, 2017.

[57] A. M. Thiebaut, M. Gauberti, C. Ali et al., "The role of plasminogen activators in stroke treatment: fibrinolysis and beyond," *The Lancet Neurology*, vol. 17, no. 12, pp. 1121–1132, 2018.